Electronic Supplementary Material (ESI) for ChemComm.
This journal is © The Royal Society of Chemistry 2015

Supplementary Information

Exact Helical Polymer Synthesis by Two-point-covalent-linking Protocol between C_2-Chiral Spirobifluorene and C_2- or C_s-Symmetric Anthraquinone Monomers

Zhaozhong Yi, Hitoshi Okuda, Yasuhito Koyama, Ryota Seto, Satoshi Uchida, Hiromitsu Sogawa, Shigeki Kuwata, Toshikazu Takata*

Department of Organic and Polymeric Materials, Tokyo Institute of Technology
2-12-1, Ookayama, Meguro, Tokyo 152-8552, Japan

Correspondence to: T. Takata (Email: ttakata@polymer.titech.ac.jp.)

1. Materials and measurements

Materials: Racemic and optically pure 2,2'-dihydroxy-9,9'-spirobifluorene **(*R*)-1**[1], and 1,5-bis(*p*-tolyloxy)anthracene-9,10-dione **4**[2] were prepared according to the literature. Other commercially available materials were used without further purification. All solvents were dried before the use if necessary.

Measurements: ^{1}H NMR (400 MHz) and ^{13}C NMR (100 MHz) spectra were recorded on a JEOL AL-400 spectrometer using $CDCl_3$ and acetone-d_6 as the solvent and tetramethylsilane as an internal standard. The molecular weights and their distributions were estimated by a size exclusion column chromatography (SEC) on a JASCO Gulliver system equipped with two consecutive linear polystyrene gel columns (Tosoh TSK-gel GMHXL and G5000HXL) at 30 °C (flow rate 0.85 mL/min) according to polystyrene standards using $CHCl_3$ as the eluent. SEC analyses were also performed using Wyatt Technology Dawn EOS-N MALS detector and Viscotek Model TDA300 on-line RI and viscometric detectors at 30 °C (flow rate 1.00 mL/min) on the basis of polystyrene standards using THF as the eluent. Right-angle scattering (RALS) information was obtained from the MALS detector and integrated into the TDA detector system to calculate the absolute molecular weights, distributions, and Mark–Houwink–Sakurada coefficients (α). FT-IR spectra were recorded on a JASCO FT/IR-460 Plus spectrophotometer. Melting points were measured with a Stuart Scientific SMP3. MALDI–TOF MS spectra were recorded on a Shimadzu Voyager-DE STR-H mass spectrometer (matrix: CHCα). UV-vis spectra were recorded on a JASCO V-550 UV-vis spectrometer. CD spectra were recorded on a JASCO J-820 spectropolarimeter. ESI–TOF MS spectra were taken on a Bruker Daltonics microTOF II mass spectrometer at the Center for Advanced Material Analysis, Tokyo Institute of Technology on request. FAB MS spectra were taken on a JMS-700 mass spectrometer at the Center for Advanced Material Analysis, Tokyo Institute of Technology on request. MALDI–TOF MS spectra were taken on an AXIMA-CFR plus mass spectrometer.

2. Experimental section

Typical procedure for intramolecular cyclization of **4** (Table S1, entry 3)

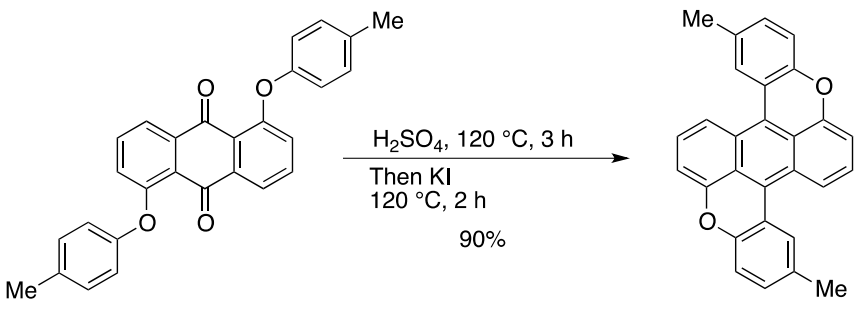

4 **5**

Table S1. Cyclization of **4**[a]

Entry	Acid	Additive	Yield of **5** (%)
1	$AlCl_3$	NaCl	37[b]
2	H_2SO_4	KI[c]	40
3	H_2SO_4	H_2O	–[d]
4	H_2SO_4	KI	90
5	H_2SO_4	Bu_4NI	88
6	CF_3SO_3H	KI	–[d]

[a] An additive was added after the reaction in acid for 2 h at 120 °C. [b] Phenol **6** was obtained as a byproduct. [c] The reaction mixture was poured into an aqueous solution of KI (1.0 M) at room temperature. [d] No reaction.

4 (50 mg, 0.12 mmol) and concd H_2SO_4 (5.0 mL) were placed in a 10 mL one-necked round-bottomed flask. The mixture was stirred at 120 °C for 3 h. After cooling to room temperature, KI (70 mg, 0.42 mmol) was added to the mixture. The mixture was stirred at 120 °C for 2 h, cooled to room temperature, and poured into a half-saturated K_2CO_3 aqueous solution. The products were extracted with CH_2Cl_2 repeatedly. The combined organic layer was washed with sat. $Na_2S_2O_3$ aq., dried over $MgSO_4$, filtered, and evaporated in vacuo. The crude product was purified by a silica gel column chromatography (eluent: hexane–CH_2Cl_2 (3:2 v/v)) to give **5** (48 mg, 90%) as a pink solid; mp 270–273 ºC (lit. 282 ºC)[2]; ^{1}H NMR (400 MHz, $CDCl_3$, 293 K) δ 8.12 (d, J = 8.7 Hz, 2H), 8.01 (s, 2H), 7.35 (dd, J = 7.6, 8.7 Hz, 2H), 7.25–7.08 (m, 4H), 6.92 (d, J = 7.6 Hz, 2H), 2.40 (s, 6H) ppm; IR (KBr) υ 3000, 1600, 1525, 1260, 780

cm^{-1}; FAB-HRMS [M]$^+$ calc'd for $C_{28}H_{19}O_2$, 386.1307; found, 386.1307; UV-vis abs. (CH_2Cl_2, 250–700 nm) 548, 510, 412, 310 nm.

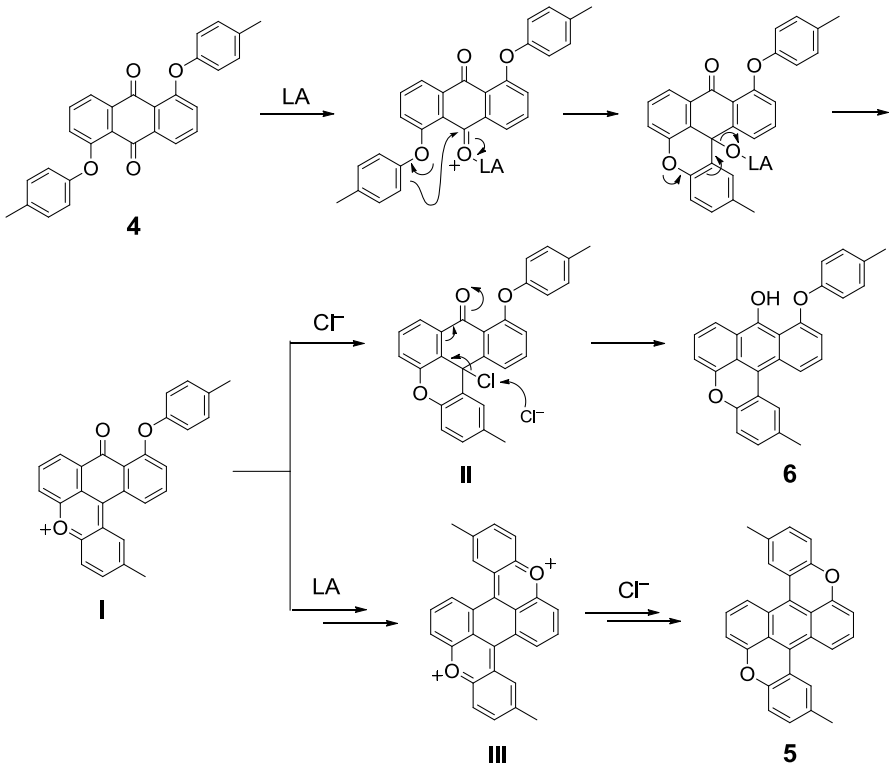

Scheme S1. Plausible mechanism to give **6** and **5** using $AlCl_3$ and NaCl.

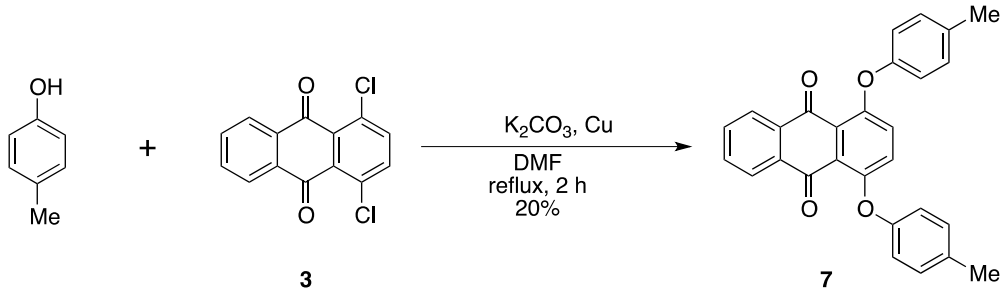

p-Cresol (3.4 mL, 33 mmol), **3** (3.0 g, 10.8 mmol), K_2CO_3 (4.5 g, 32.5 mmol), Cu (1.0 g, 16.2 mmol), and DMF (10 mL) were placed in a round-bottom flask, and the mixture was refluxed for 2 h. After cooling to room temperature, 1 M NaOH aq. was added to the reaction mixture. The products were extracted with CH_2Cl_2. The combined organic layer was dried over $MgSO_4$, filtered, and evaporated in vacuo. The crude product was purified by a silica gel column chromatography (eluent: hexane–ethyl acetate (1:1 v/v)) to give **7** as an orange solid. The analytically pure sample **7** (0.90 g, 20%) was obtained by recrystallization using CH_2Cl_2–hexane; mp 193.8–194.3 ºC; ^{1}H NMR (400 MHz, Acetone-d_6, 298 K) δ 7.96 (ddd, J = 3.4, 3.3,

2.4 Hz, 2H), 7.72 (ddd, J = 3.4, 3.3, 2.4 Hz, 2H), 7.28 (s, 2H), 7.05 (d, J = 8.0 Hz, 4H), 6.81 (d, J = 8.0 Hz, 4H), 2.17 (s, 6H) ppm; IR (KBr) υ 3000, 1670, 1260, 798 cm^{-1}; ^{13}C NMR (100 MHz, $CDCl_3$, 293 K) δ 182.1, 154.6, 153.0, 134.0, 134.0, 133.6, 130.4, 127.8, 126.7, 125.3, 118.1, 20.6 ppm; UV-vis abs. (CH_2Cl_2, 250–700 nm) 375 nm; $[M]^+$ calc'd for $C_{28}H_{20}O_4$, 420.1362; found, 420.1358.

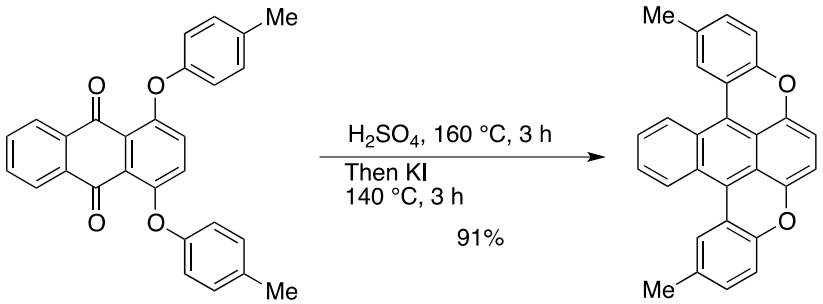

7 **8**

7 (50 mg, 0.12 mmol) and concd H_2SO_4 (5.0 mL) were placed in a 10 mL one-necked round-bottomed flask, and the mixture was stirred at 160 °C for 3 h. After cooling to room temperature, KI (70 mg, 0.42 mmol) was added to the mixture. The mixture was stirred at 140 °C for 3 h, cooled to room temperature, and poured into a half-saturated K_2CO_3 aqueous solution. The products were extracted with CH_2Cl_2. The combined organic layer was washed with sat. $Na_2S_2O_3$ aq., dried over $MgSO_4$, filtered, and evaporated in vacuo to give **8** (49 mg, 91%) as a pink solid with a trace amount of the endoperoxide; mp 173.8–175.4 °C; ^1H NMR (400 MHz, Acetone-d_6, 298 K) δ 8.49–8.47 (m, 2H), 7.74 (s, 2H), 7.42–7.40 (m, 2H), 7.05 (d, J = 8.3 Hz, 2H), 6.89 (d, J = 8.3 Hz, 2H), 6.62 (s, 2H), 2.26 (s, 6H) ppm; ^{13}C NMR (100 MHz, $CDCl_3$, 293 K) δ 153.5, 144.9, 132.5, 130.2, 128.1, 127.7, 126.3, 126.1, 123.2, 122.3, 122.1, 116.8, 105.9, 21.2 ppm; IR (KBr) υ 2917, 2848, 1462, 1260, 1100, 803 cm^{-1}; FAB-HRMS $[M]^+$ calc'd for $C_{28}H_{19}O_2$, 386.1307; found, 386.1310.

Synthesis of model compound **10**

We investigated the reductive cyclization of **9** possessing *o*-formyl phenyl ethers to confirm the cyclization position of the SBF moiety, because the SBF skeleton has two reactive points at the 1- and 3-positions (Scheme S2). Ultimately, the reductive cyclization of **9** proceeded even when using CF_3SO_3H to afford 3-position-fused xanthene **10** selectively. The structure of **10** was determined with ^{1}H NMR, ^{13}C NMR, FT-IR, and single crystal X-ray analysis. These results indicate that the cyclization at the 3-position of SBF is remarkably faster than that at the 1-position, probably due to steric hindrance around the latter position.

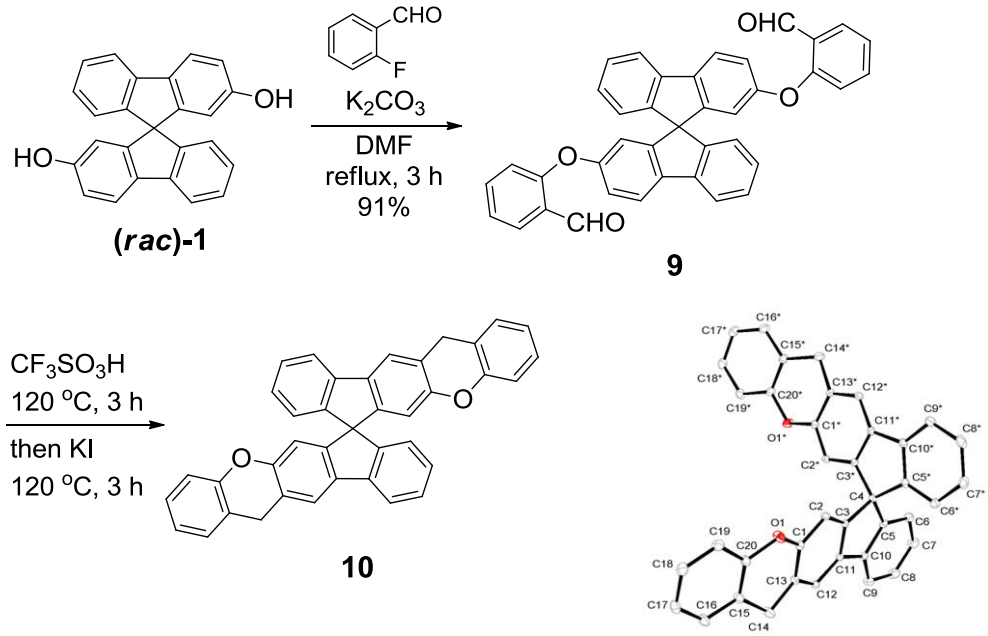

Scheme S2. Synthesis and ORTEP diagram of model compound **10**. Hydrogen atoms are omitted for clarity. Thermal ellipsoids at 50% probability.

(*rac*)-1 (500 mg, 1.40 mmol), 2-fluorobenzaldehyde (450 mg, 3.59 mmol), K_2CO_3 (500 mg, 3.59 mmol), and DMF (10 mL) were placed in a round-bottom flask, then the mixture was refluxed for 3 h. The reaction mixture was cooled to room temperature, diluted with CH_2Cl_2, dried over $MgSO_4$, filtered, and evaporated in vacuo. The crude product was purified by a silica gel column chromatography (eluent: hexane–CH_2Cl_2 (1:1 v/v)) to give **9** (720 mg, 90%) as a white solid; mp 112.4–114.2 °C; ^{1}H NMR (400 MHz, Acetone-d_6, 298 K) δ 10.35 (s, 2H), 8.01 (d, J = 8.3 Hz, 2H), 7.93 (d, J = 7.6 Hz, 2H), 7.78 (d, J = 7.8 Hz, 2H), 7.53 (dd, J = 7.6, 7.3 Hz, 2H), 7.40 (dd, J = 7.6, 7.6 Hz, 2H), 7.20–7.12 (m, 6H), 6.82 (d, J = 8.3 Hz, 2H), 6.71 (d, J = 7.8 Hz, 2H), 6.54 (s, 2H) ppm; ^{13}C NMR (100 MHz, $CDCl_3$, 293 K) δ 189.1, 160.7, 157.2,

151.6, 149.1, 141.8, 139.1, 136.6, 129.0, 128.8, 128.6, 127.5, 124.4, 124.2, 122.7, 121.0, 120.4, 118.9, 116.0, 66.0 ppm; IR (KBr) υ 3044, 2857, 1685, 1449, 1219, 756 cm^{-1}; FAB HR-MS $[M]^+$ calc'd for $C_{39}H_{24}O_4$, 565.1675; found, 556.1658.

9 (100 mg, 0.18 mmol) and CF_3SO_3H (5.0 mL) were placed in a 10 mL one-necked round-bottomed flask, and the mixture was stirred at 120 °C for 3 h. After cooling the reaction mixture to room temperature, KI (70 mg, 0.42 mmol) was added to the mixture. The mixture was stirred at 120 °C for 3 h, cooled to room temperature, and poured into a half-saturated K_2CO_3 aqueous solution. The products were extracted with CH_2Cl_2. The combined organic layer was washed with sat. $Na_2S_2O_3$ aq., water, and brine, dried over $MgSO_4$, filtered, and evaporated in vacuo. The crude product was purified by a silica gel column chromatography (eluent: hexane–CH_2Cl_2 (2:1 v/v)) and recrystallized from acetone to give an analytically pure sample **10** (28 mg, 28%) as a pale yellow solid; mp 116.8–118.2 °C; ^{1}H NMR (400 MHz, Acetone-d_6, 298 K) δ 7.81 (d, J = 7.6 Hz, 2H), 7.72 (s, 2H), 7.27 (dd, J = 7.3, 7.6 Hz, 2H), 7.13 (d, J = 7.6 Hz, 2H), 7.03–6.96 (m, 4H), 6.89 (dd, J = 7.3, 7.3 Hz, 2H), 6.74 (d, J = 8.3 Hz, 2H), 6.56 (d, J = 7.6 Hz, 2H), 6.22 (s, 2H), 4.05 (s, 4H) ppm; ^{13}C NMR (100 MHz, $CDCl_3$, 298 K) δ 152.2, 152.1, 149.0 148.8, 141.5, 136.9, 128.9, 128.0, 127.7, 127.3, 124.2, 123.1, 120.5, 120.5, 120.2, 119.6, 116.5, 112.4, 65.7, 28.6; IR(KBr) υ 2924, 1577, 1481, 1447, 1359, 1266, 1234, 1103, 872, 753 cm^{-1}; FAB HR-MS $[M]^+$ calc'd for $C_{39}H_{24}O_2$, 524.1776; found, 524.1785; Crystals of **7** suitable for X-ray analysis were obtained by recrystallization from a solution of acetone. Single crystal data of **7**·(acetone)$_2$: $C_{45}H_{36}O_4$, M_w = 640.78, pale yellow, size: 0.37 × 0.26 × 0.15 mm, monoclinic, C2/c (#15), Z = 4, a = 20.810(5) Å, b = 13.789(3) Å, c = 12.317(3) Å, β = 90.752(4)°, V = 3534(2) Å^3, D_{calc} = 1.204 g/cm^3, μ = 0.757 cm^{-1}, T = 113 K, F(000) = 1352, Rigaku Saturn CCD area detector with graphite monochromated Mo Kα radiation (λ = 0.7107 Å), 14220 reflections measured, 4024 unique reflections (R_{int} = 0.0379). Refined parameters, final $R1$ = 0.0549 for reflections with $I > 2\sigma(I)$, wR = 0.1343 (all data), GOF = 1.000. Final largest diffraction peak and hole: 0.51 and –0.33 e^-/Å^3. Crystallographic data reported in this manuscript have been deposited with Cambridge Crystallographic Data Centre as supplementary publication no. CCDC-960052.

Typical procedure for polymerization of **(*R*)-1** and **2** (Table S2, Entry 2)

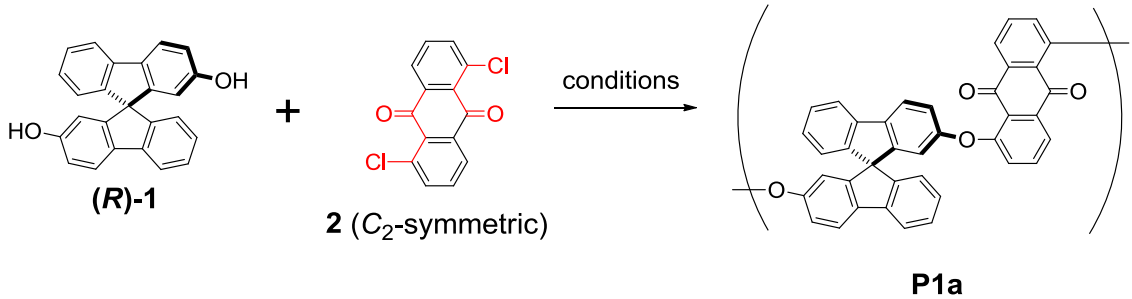

Table S2. Effects of temperature and base on polycondensation of **(*R*)-1** and **2**.

Entry	Solvent	Base	Temp. (°C)	Yield (%)	M_n[a] (× 10^3)	M_w/M_n[a]
1	DMF	K_2CO_3	160	87	4.0	1.8
2	DPS	K_2CO_3	210	86	9.0	2.6
3	DPS	Cs_2CO_3	210	20	3.0	4.2

[a] Estimated by SEC on a basis of polystyrene standards in DMF containing LiBr (0.01 M). DMF = *N*,*N*-dimethylformamide, DPS = diphenylsulfone.

(*R*)-1 (0.10 g, 0.29 mmol), **2** (80 mg, 0.29 mmol), K_2CO_3 (90 mg, 0.86 mmol), and diphenylsulfone (DPS, 1.5 g) were placed in a round-bottom flask, and the mixture was stirred at 160 °C for 5 h. After cooling to room temperature, the reaction mixture was diluted with CH_2Cl_2 to give inorganic precipitates. The precipitates were removed by filtration. The filtrate was poured into MeOH to give an yellow solid, which was collected by filtration, washed with MeOH, and dried in vacuo to give **P1a** (137 mg, 86%) as an yellow solid; M_w 9000, M_w/M_n 2.6 (estimated by SEC on the basis of polystyrene standards using $CHCl_3$ as an eluent); M_w 14600, M_w/M_n 2.0, α 0.07 (estimated by SEC-VISC-RALS on the basis of polystyrene standards using THF as an eluent); no T_g was observed in a range from room temperature to 200 ºC; T_{d5} 324.9 ºC; ^{1}H NMR (400 MHz, $CDCl_3$, 293 K) δ 7.88–7.85 (m, 2H), 7.78–7.72 (m, 4H), 7.75–7.49 (m, 2H), 7.32–7.30 (m, 2H), 7.10–6.96 (m, 6H), 6.76–6.74 (m, 2H), 6.57 (s, 2H) ppm; IR (KBr) υ 3326, 3063, 1674, 1581, 1445, 1244, 734 cm^{-1}; UV-vis abs. (CH_2Cl_2, 250–700 nm) 375, 315 nm.

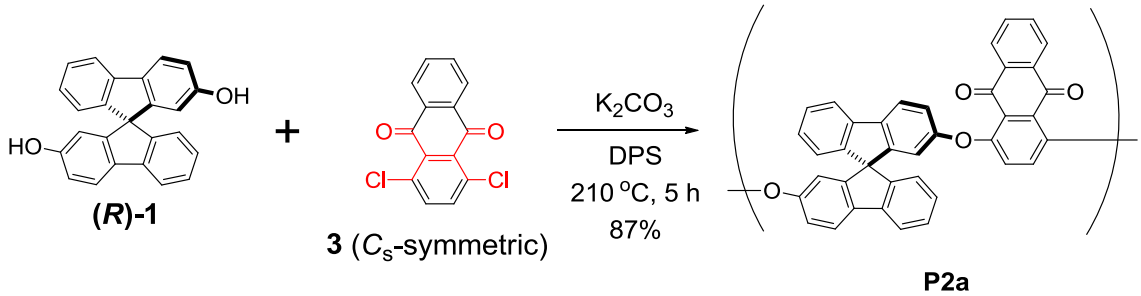

(*R*)-1 (0.20 g, 0.57 mmol), **3** (0.16 g, 0.57 mmol), K_2CO_3 (170 g, 1.25 mmol), and diphenylsulfone (1.0 g) were placed in round-bottom flask, and the mixture was stirred at 210 °C for 5 h. After cooling to room temperature, the reaction mixture was diluted with CH_2Cl_2 to give inorganic precipitates. The precipitates were removed by filtration. The filtrate was poured into MeOH to give an yellow solid, which was collected by filtration, washed with MeOH, and dried in vacuo to give **P2a** (139 mg, 87%) as an yellow solid; M_w 8000, M_w/M_n 2.4 (estimated by SEC on the basis of polystyrene standards using $CHCl_3$ as an eluent); M_w 6700, M_w/M_n 1.8, α 0.29 (estimated by SEC-VISC-RALS on the basis of polystyrene standards using THF as an eluent); no T_g was observed in a range from room temperature to 200 °C; T_{d5} 375.2 °C; ^{1}H NMR (400 MHz, $CDCl_3$ 298 K) δ 8.00–7.90 (m, 2H), 7.68–7.65 (m, 4H), 7.51–7.48 (m, 2H), 7.31–7.20 (m, 2H), 7.08 (s, 2H), 6.99–6.91 (m, 2H), 6.85–6.82 (m, 2H), 6.73–6.66 (m, 2H), 6.51(s, 2H) ppm; IR (KBr) υ 3057, 1675, 1444, 1236, 726 cm^{-1}; UV-vis abs. (CH_2Cl_2, 200–700 nm) 400 nm.

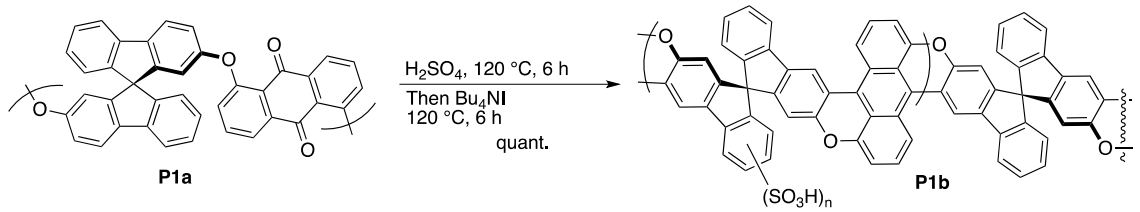

P1a (50 mg, 0.090 mmol) and concd H_2SO_4 (5.0 mL) were placed in a 10 mL one-necked round-bottomed flask, and the mixture was stirred at 120 °C for 6 h. After cooling the reaction mixture to room temperature, Bu_4NI (0.20 g, 0.54 mml) was added to the mixture. The mixture was stirred at 120 °C for 6 h, cooled to room temperature, and poured into Et_2O. The purple precipitates were collected by filtration, washed with acetonitrile, acetone, and CH_2Cl_2, and dried in vacuo to give **P1b** (45 mg). From the result of the elemental analysis (found: C, 55.25; H, 3.65; S, 7.30), we determined the functionalization ratio of SO_3H to be 1.9 per one repeating unit; IR (KBr) υ 3000, 1190, 1010 cm^{-1}.

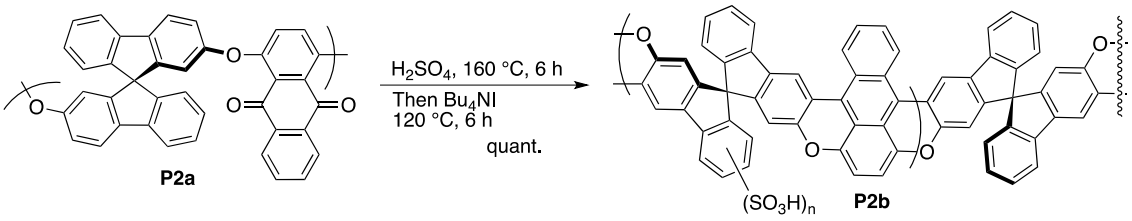

P2a (50 mg, 0.090 mmol) and concd H_2SO_4 (5.0 mL) were placed in a 10 mL one-necked round-bottomed flask, and the mixture was stirred at 160 °C for 6 h. After cooling the reaction mixture to room temperature, Bu_4NI (0.20 g, 0.54 mml) was added to the mixture. The mixture was stirred at 120 °C for 6 h, cooled to room temperature, and poured into Et_2O. The purple precipitates were collected by filtration, washed with acetonitrile, acetone, and CH_2Cl_2, and dried in vacuo to give **P2b** (48 mg). From the result of the elemental analysis (found: C, 48.58; H, 3.16; S, 3.18), we determined the functionalization ratio of SO_3H to be 2.5 per one repeating unit; IR (KBr) υ 3000, 1190, 1010 cm^{-1}.

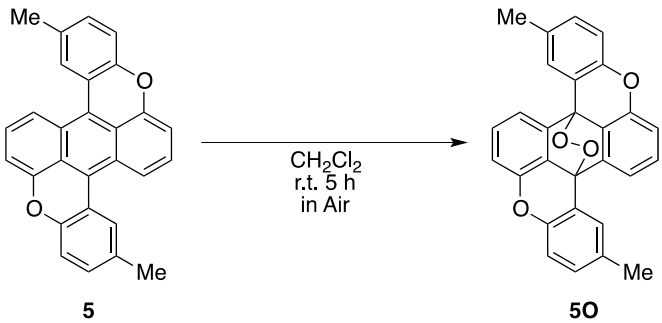

5 (5.0 mg, 0.01 mmol) and CH_2Cl_2 (5.0 mL) were placed in round-bottom flask, and the mixture was stirred for 5 h at room temperature and concentrated in vacuo to give the crude product **5O** in a quantitative yield; ^{1}H NMR (400 MHz, Acetone-d_6, 293 K) δ 7.48 (s, 2H), 7.38 (dd, J = 1.7, 8.5 Hz, 2H), 7.29 – 7.21 (m, 4H), 7.05 (d, J = 8.2 Hz, 2H), 6.86 (d, J = 7.6 Hz, 2H), 2.34 (s, 6H) ppm; IR (KBr) υ 3000, 1640, 1260, 790 cm^{-1}; UV-vis abs. (CH_2Cl_2, 200–700 nm) 315 nm; FAB-HRMS $[M]^+$ calc'd for $C_{28}H_{18}O_4$, 418.1205; found, 418.1186.

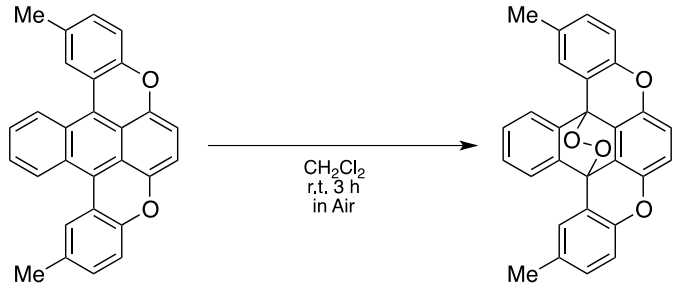

8 **8O**

8 (50 mg, 0.13 mmol) and CH_2Cl_2 (500 mL) were placed in a round-bottom flask, and the mixture was stirred for 3 h at room temperature and concentrated in vacuo to give the crude product **8O** in a quantitative yield. The crude was purified by a silica gel column chromatography (eluent: hexane–$CHCl_3$ (1:1 v/v)) to give **8O** (10 mg, 18%) as a pale yellow solid; mp 142 °C (decomp); ^{1}H NMR (400 MHz, Acetone-d_6, 298 K) δ 7.55 (d, J = 1.0 Hz, 2H), 7.39 (dd, J = 1.7, 8.6 Hz, 2H), 7.25–7.19 (m, 6H), 7.12 (s, 2H), 2.36 (s, 6H) ppm; ^{13}C NMR (100 MHz, $CDCl_3$, 298 K) δ 151.5, 142.7 140.5, 133.3, 132.8, 131.0, 127.3, 123.2, 120.2, 118.2, 116.2, 112.2, 75.0, 21.0 ppm; IR (KBr) υ 2925, 2852, 1654, 1473, 1260, 1232, 1210, 1052, 814, 743 cm^{-1}.

3. ^{1}H NMR, ^{13}C NMR, FT-IR, and MALDI−TOF MS spectra and GPC and TGA profiles

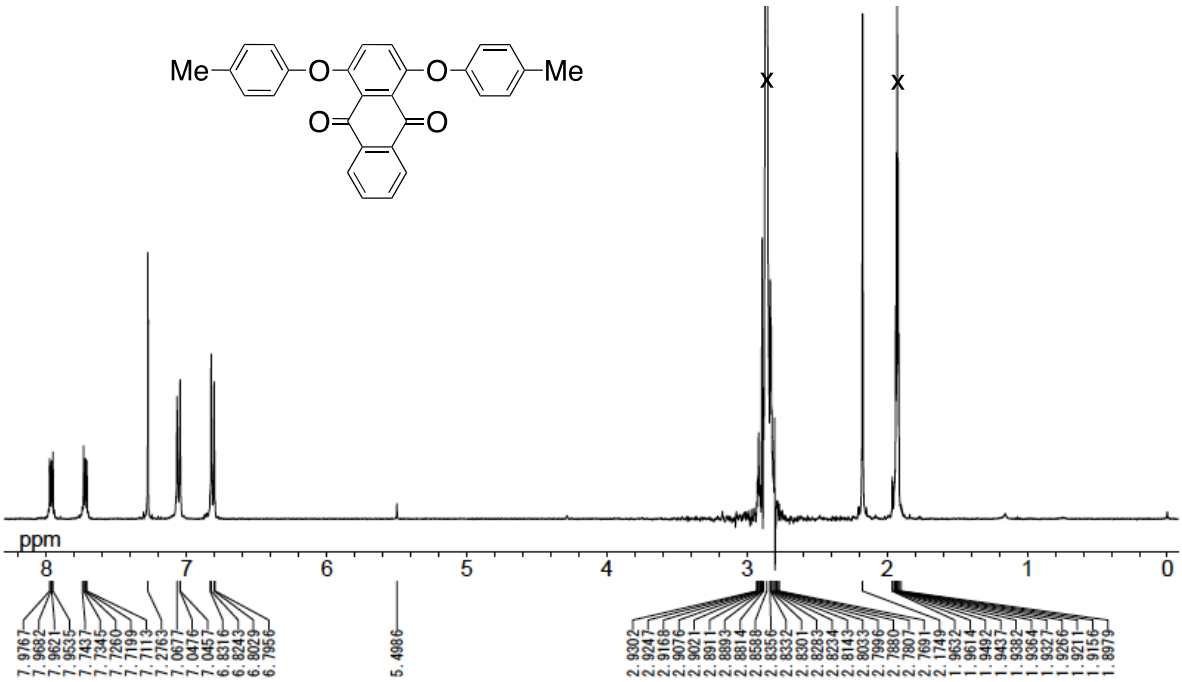

Figure S1. ^{1}H NMR spectrum of **7** (Acetone-d_6, 400 MHz, 293 K)

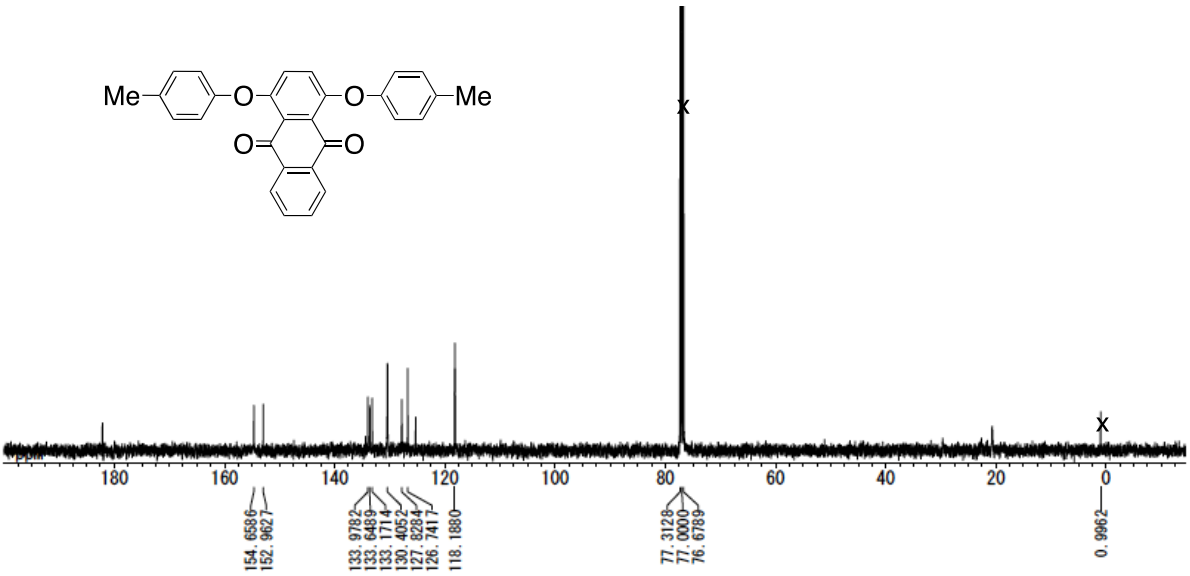

Figure S2. ^{13}C NMR spectrum of **7** ($CDCl_3$, 100 MHz, 293 K)

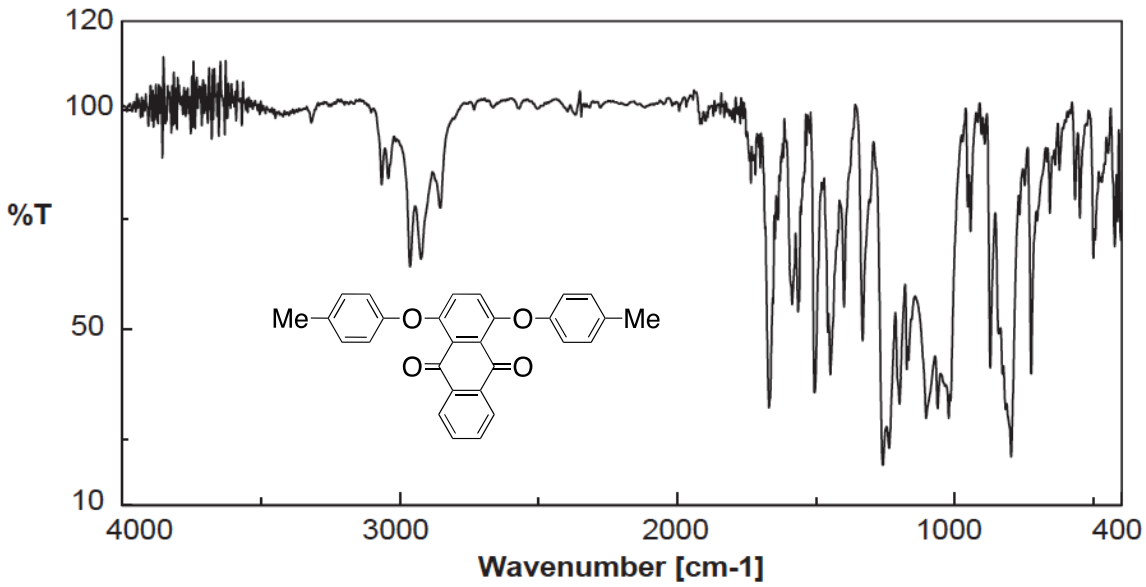

Figure S3. IR spectrum of **7** (KBr)

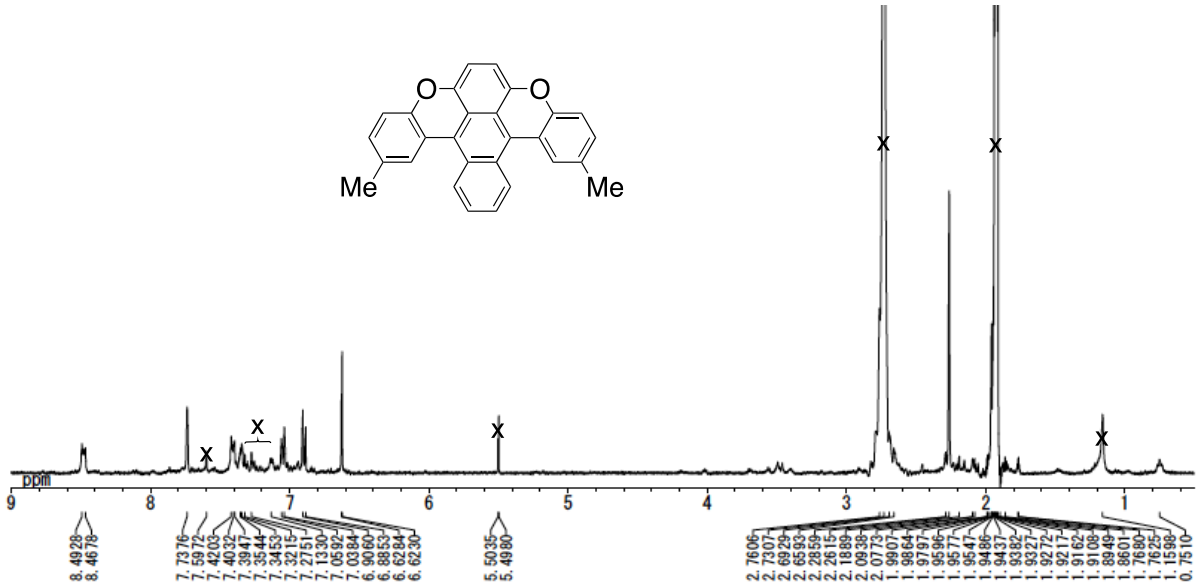

Figure S4. ^{1}H NMR spectrum of **8** (Acetone-d_6, 400 MHz, 293 K)

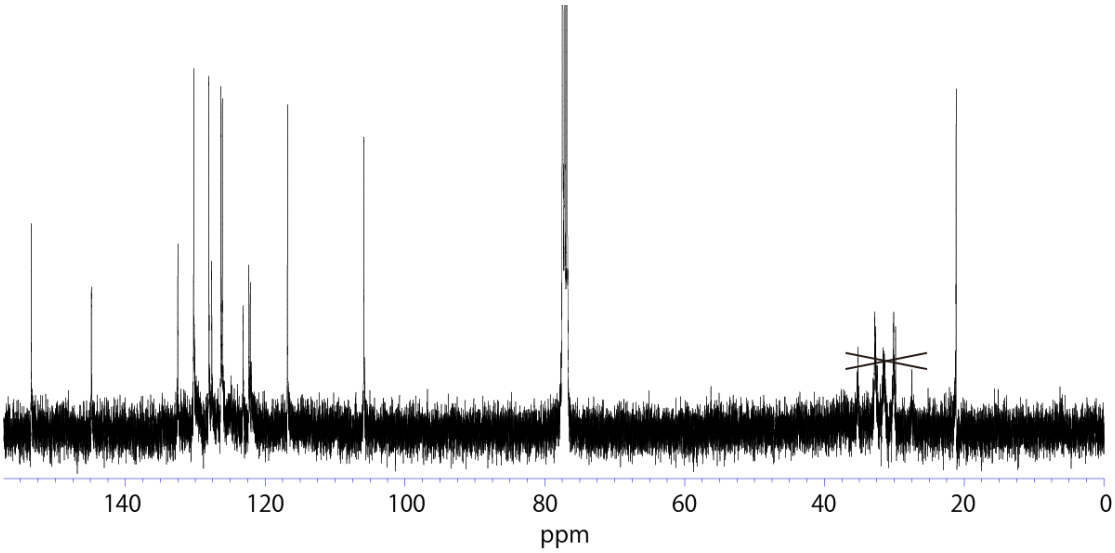

Figure S5. ^{13}C NMR spectrum of **8** (Acetone-d_6, 100 MHz, 293 K)

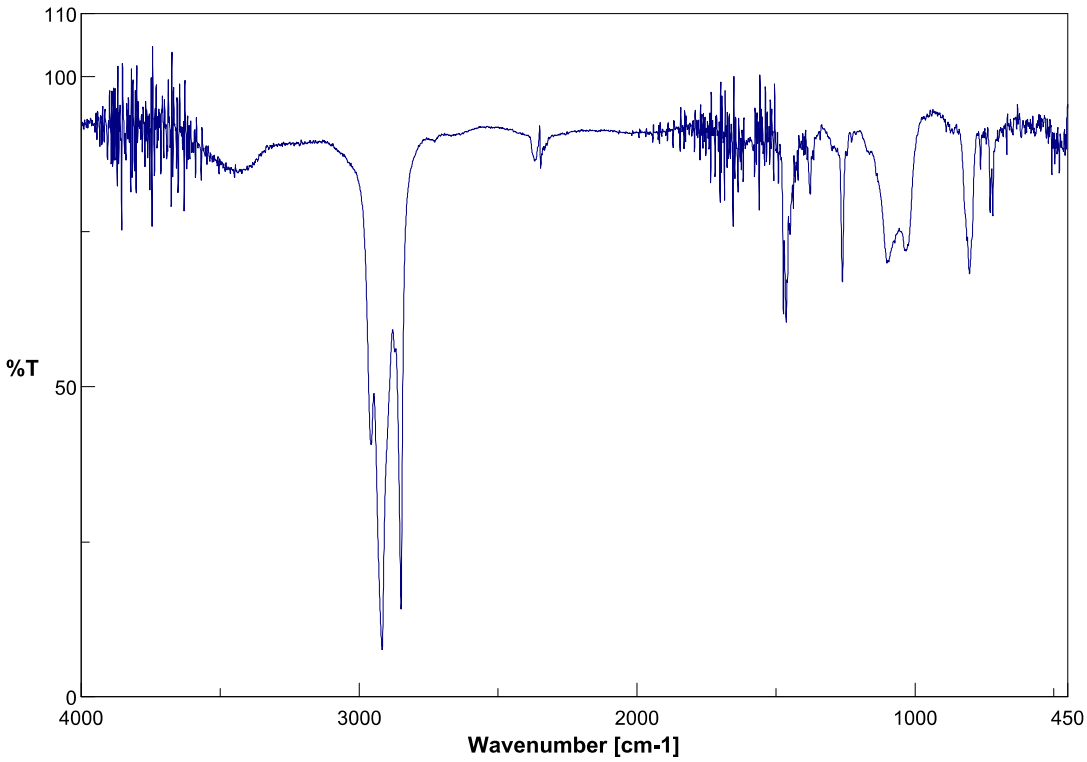

Figure S6. IR spectrum of **8** (KBr)

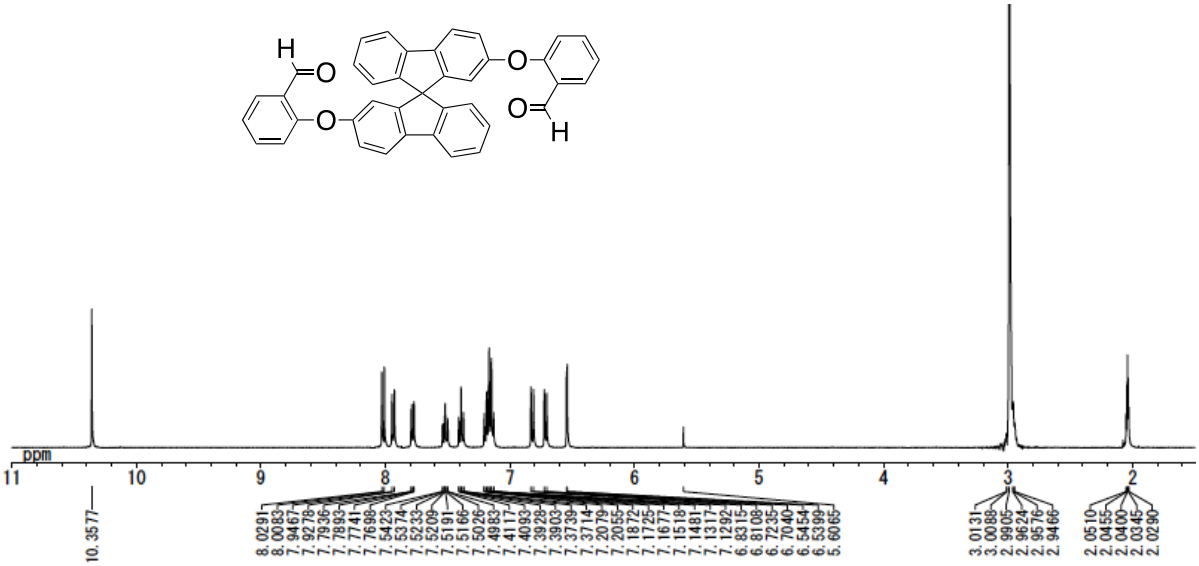

Figure S7. ^{1}H NMR spectrum of **9** (Acetone-d_6, 400 MHz, 293 K)

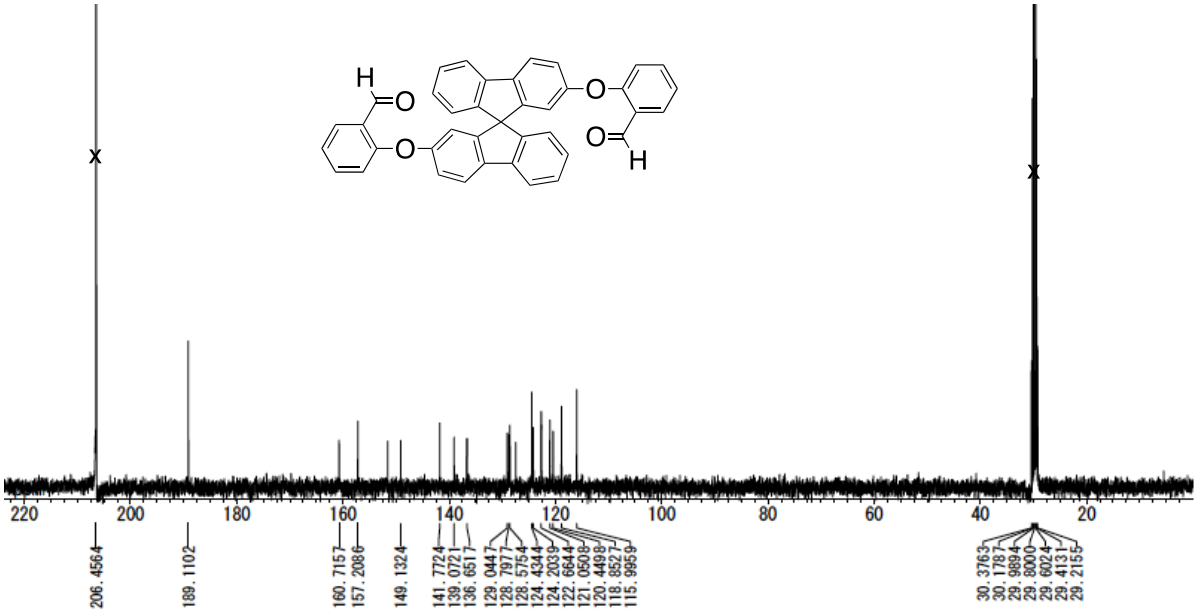

Figure S8. ^{13}C NMR spectrum of **9** (Acetone-d_6, 100 MHz, 293 K)

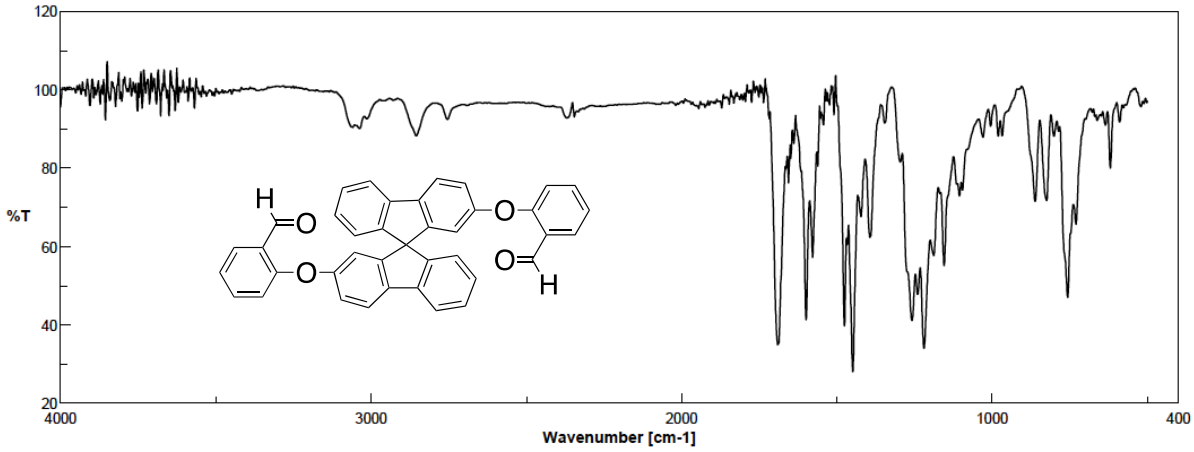

Figure S9. IR spectrum of **9** (KBr)

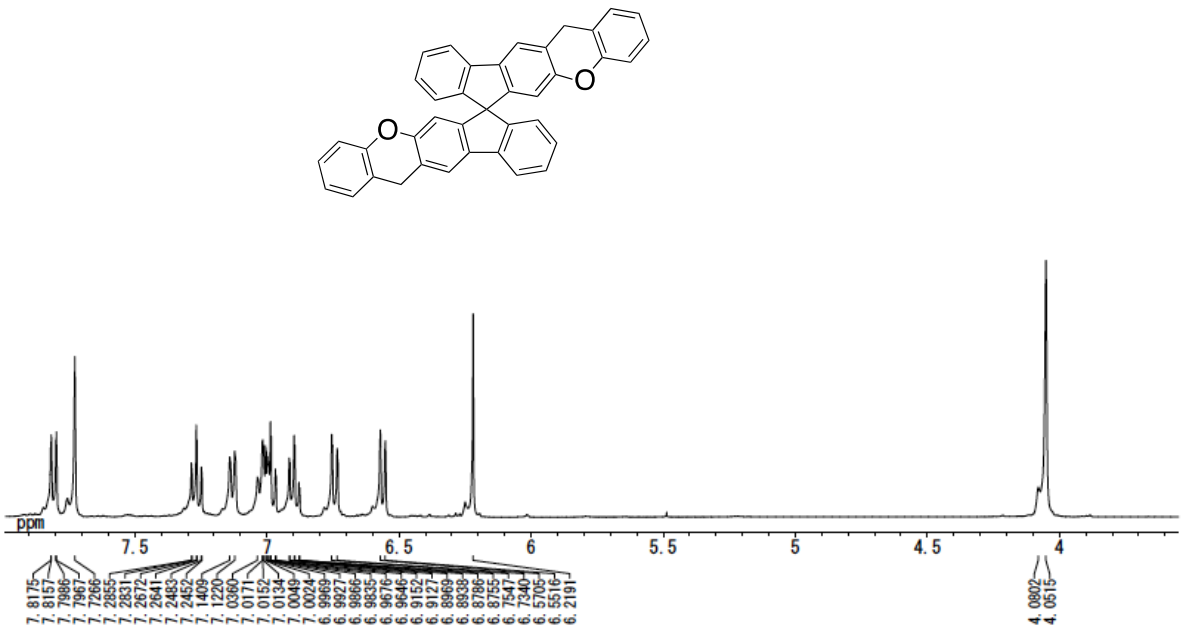

Figure S10. ^{1}H NMR spectrum of **10** (Acetone-d_6, 400 MHz, 293 K)

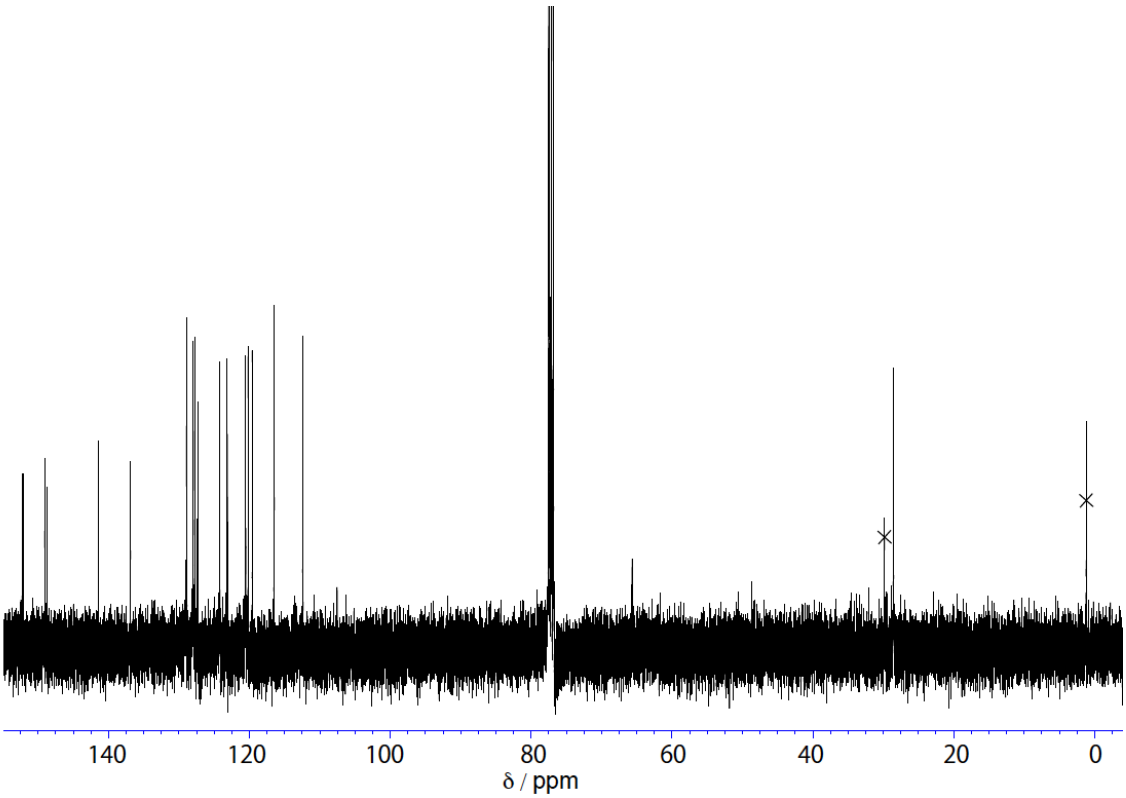

Figure S11. ^{13}C NMR spectrum of **10** ($CDCl_3$, 400 MHz, 293 K)

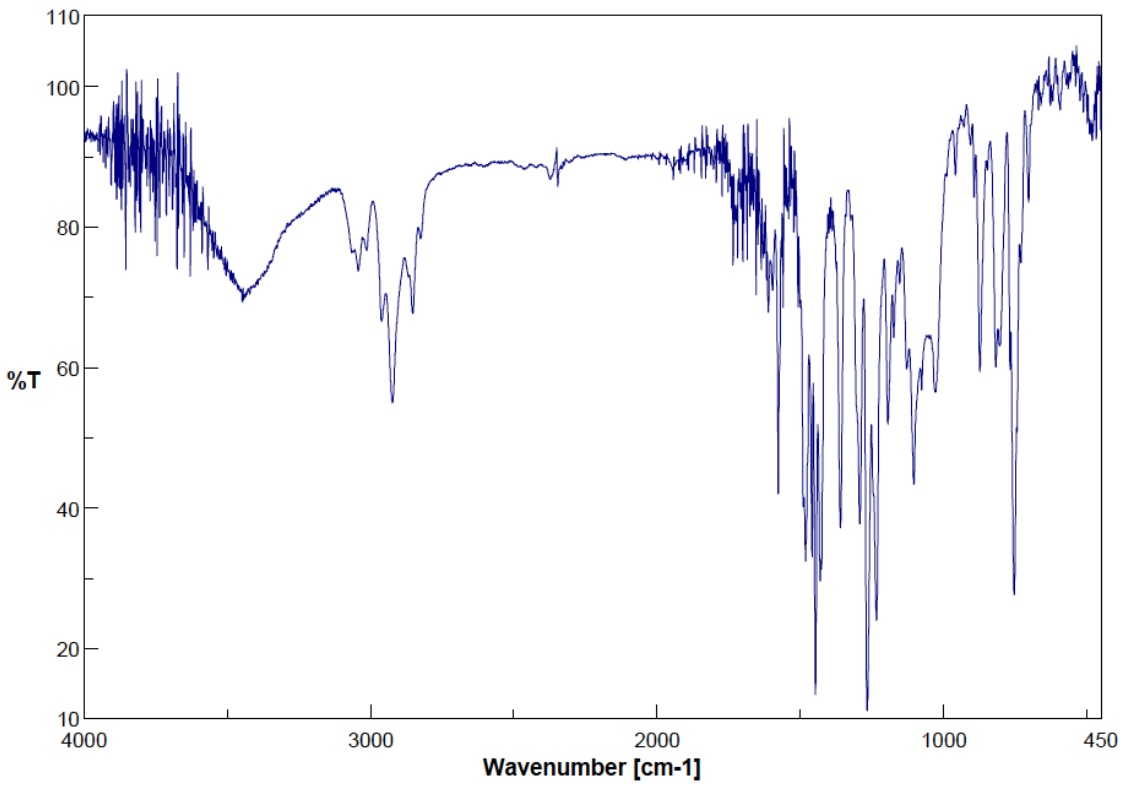

Figure S12. IR spectrum (KBr) of **10**.

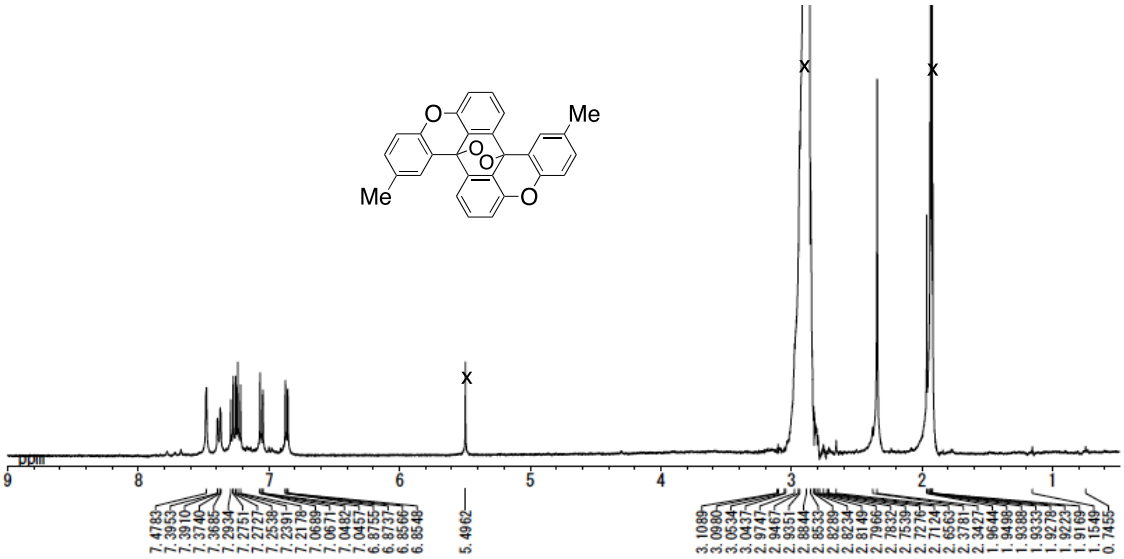

Figure S13. ^{1}H NMR spectrum of **5O** (Acetone-d_6, 400 MHz, 293 K)

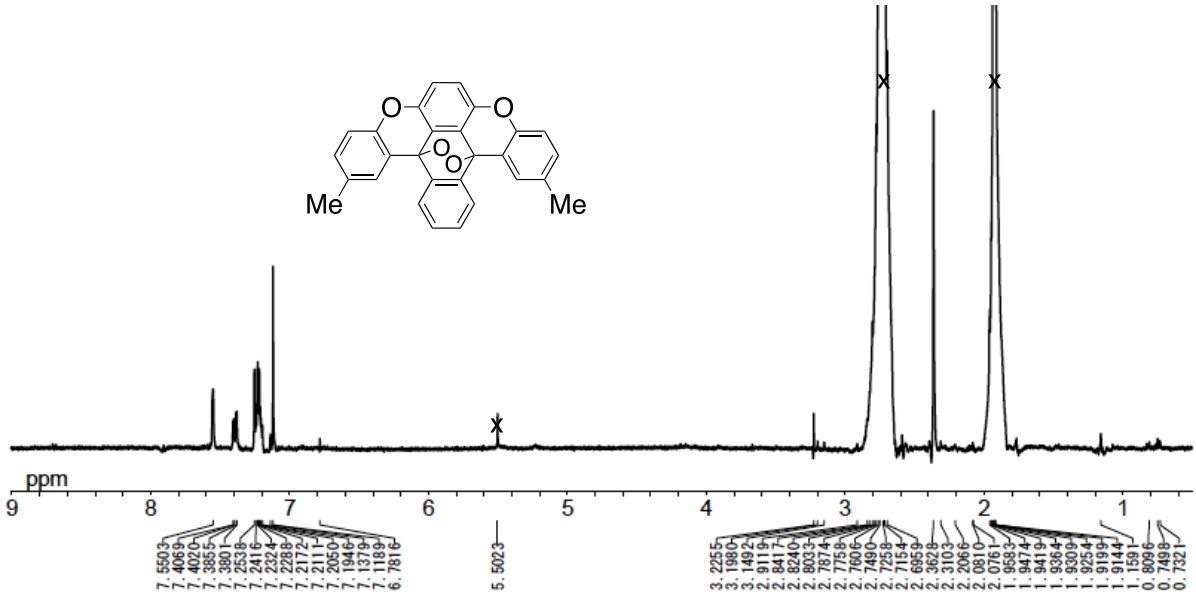

Figure S14. ^{1}H NMR spectrum of **8O** (Acetone-d_6, 400 MHz, 293 K)

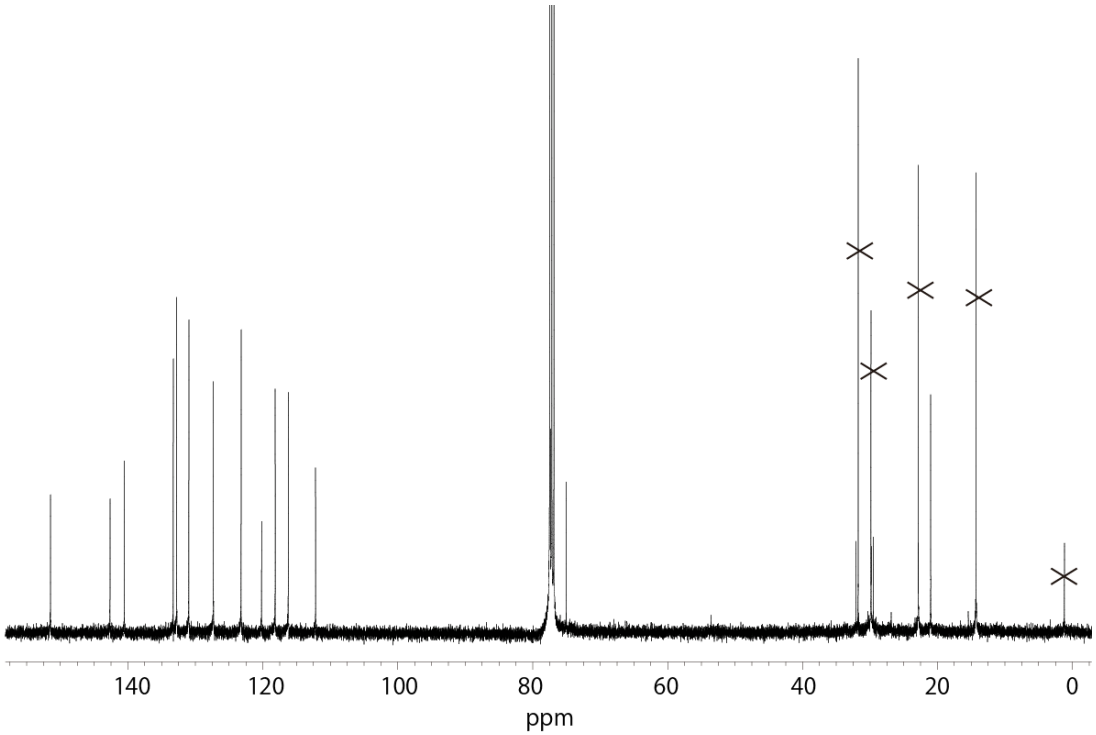

Figure S15. ^{13}C NMR spectrum of **8O** ($CDCl_3$, 400 MHz, 293 K)

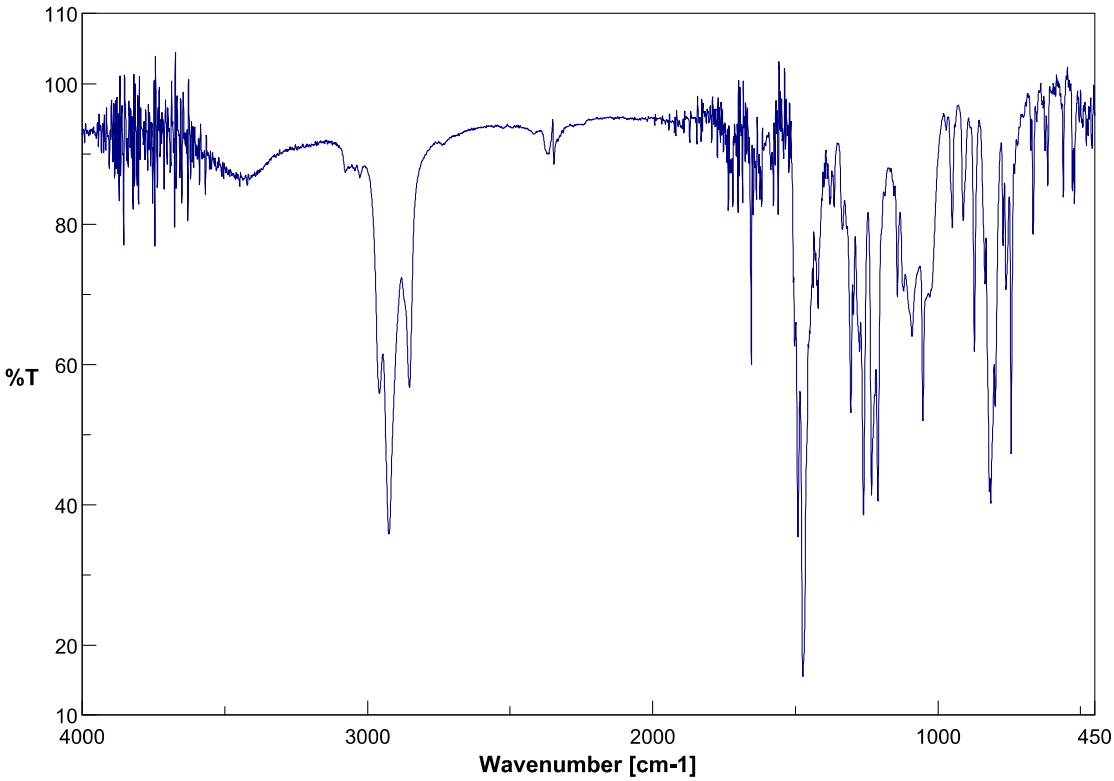

Figure S16. IR spectrum of **8O** (KBr)

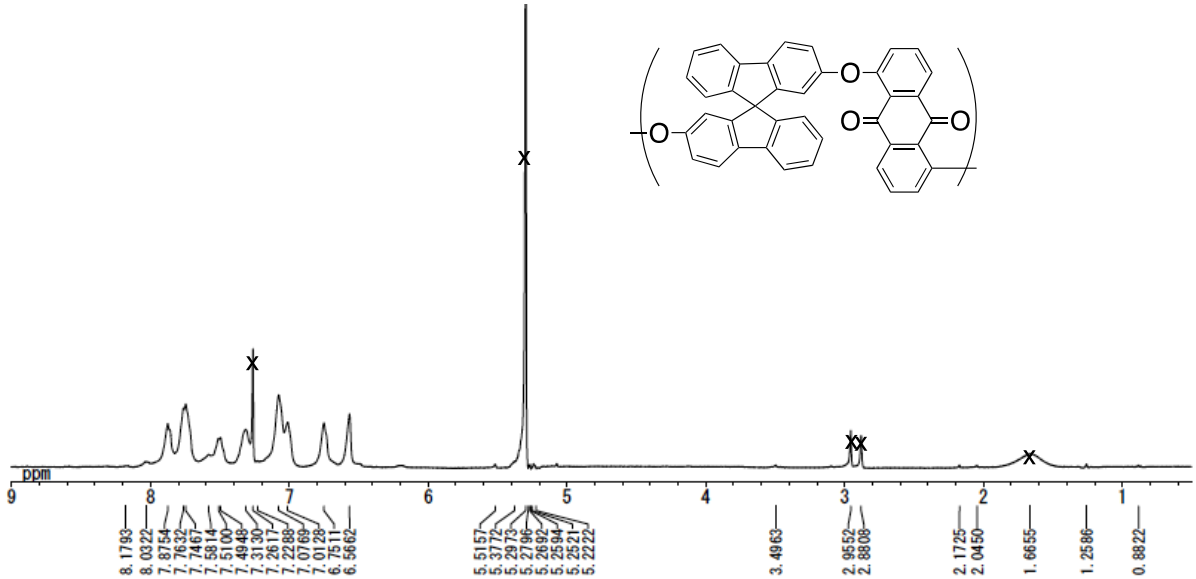

Figure S17. ^{1}H NMR spectrum of **P1a** ($CDCl_3$, 400 MHz, 293 K)

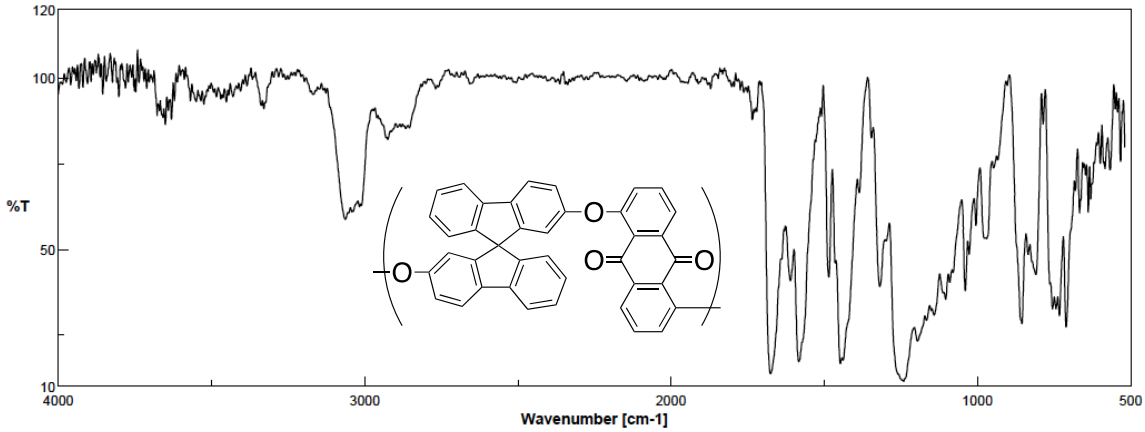

Figure S18. IR spectrum of **P1a** (KBr)

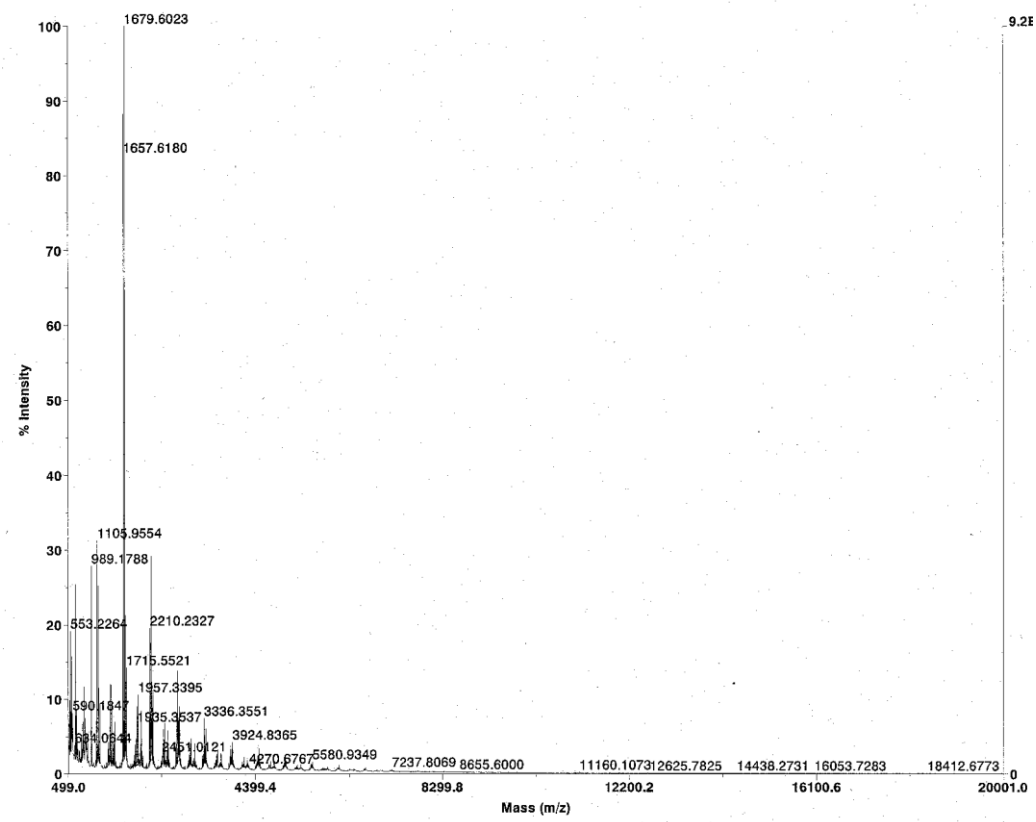

Figure S19. MALDI–TOF MS spectrum of **P1a**.

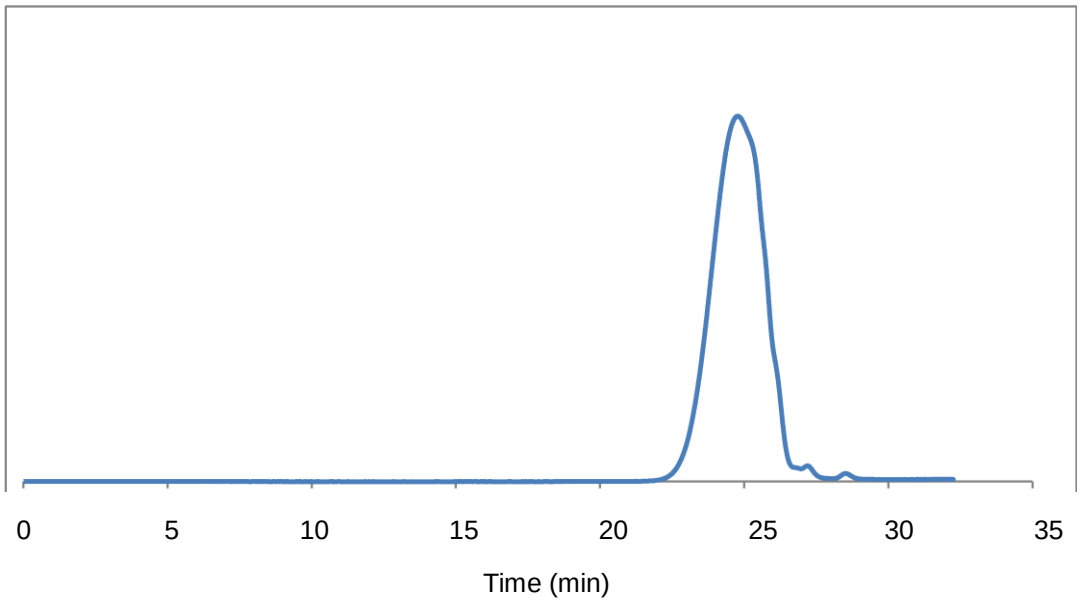

Figure S20. SEC profile of **P1a** (eluent: $CHCl_3$, 293 K)

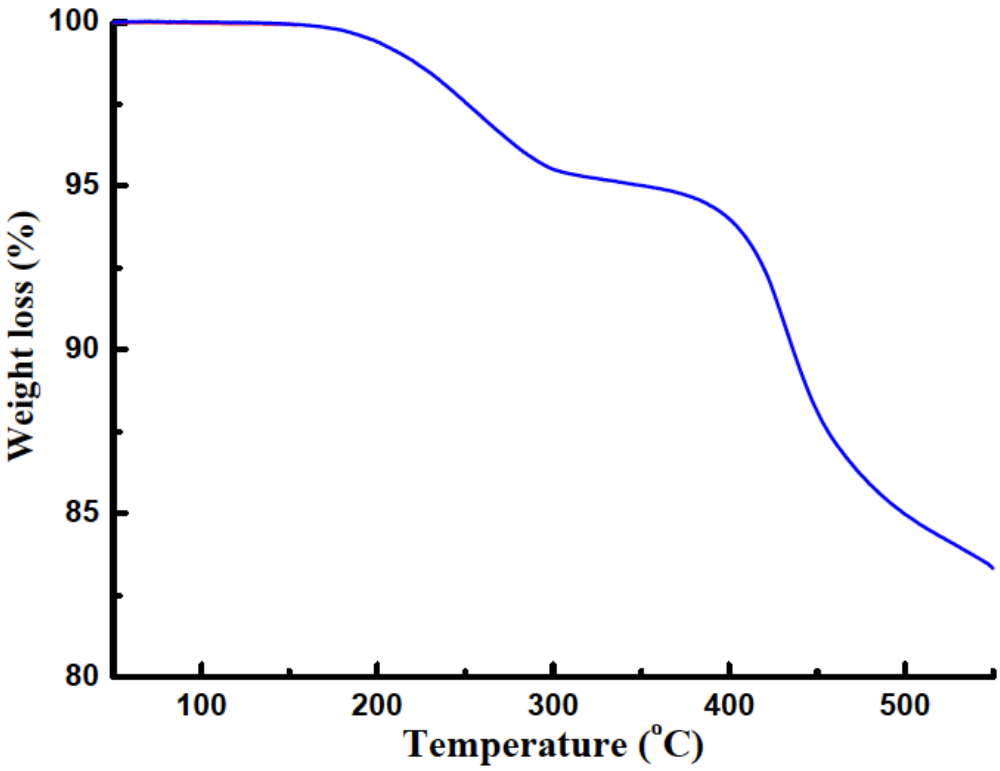

Figure S21. TGA profile of **P1a**; heating rate: 10 ºC/min; N_2 atmosphere

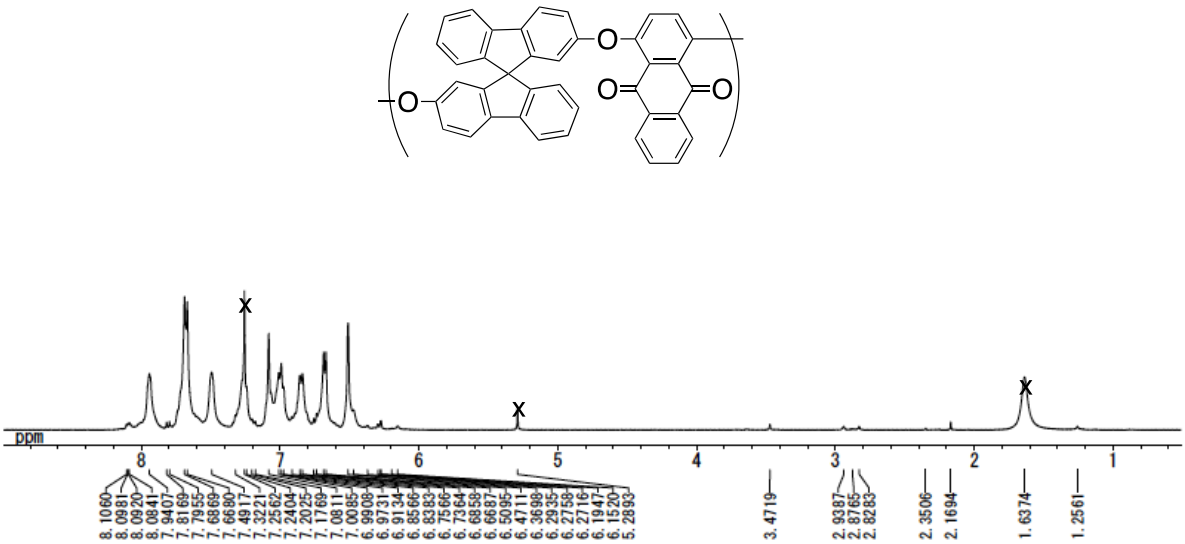

Figure S22. ^{1}H NMR spectrum of **P2a** ($CDCl_3$, 400 MHz, 293 K)

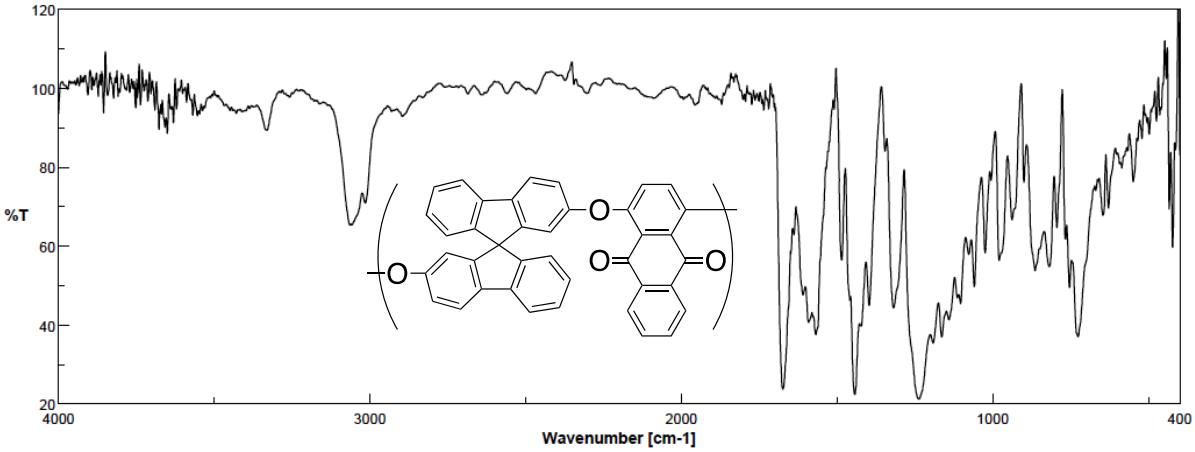

Figure S23. IR spectrum of **P2a** (KBr)

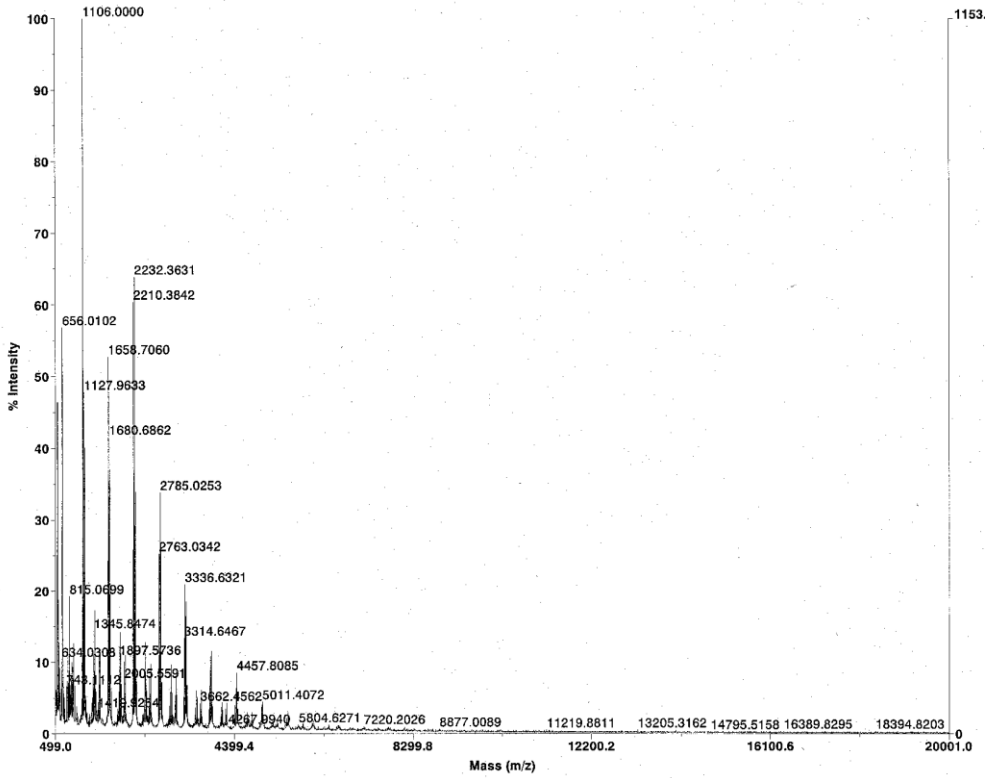

Figure S24. MALDI−TOF MS spectrum of **P2a**.

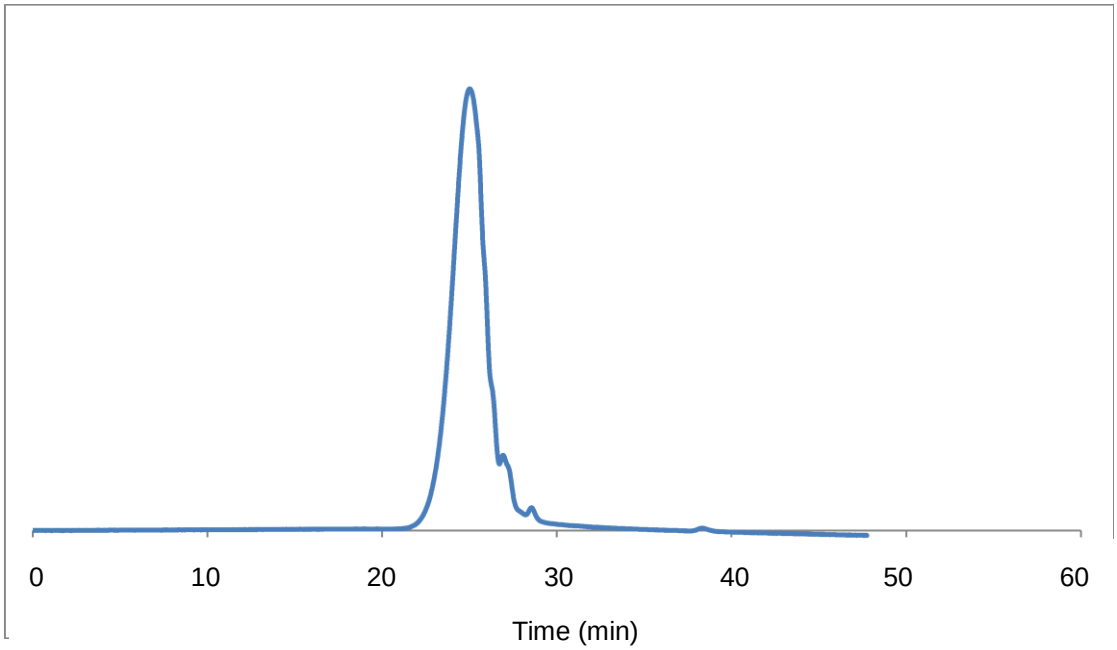

Figure S25. SEC profile of **P2a** (eluent: $CHCl_3$, 293 K)

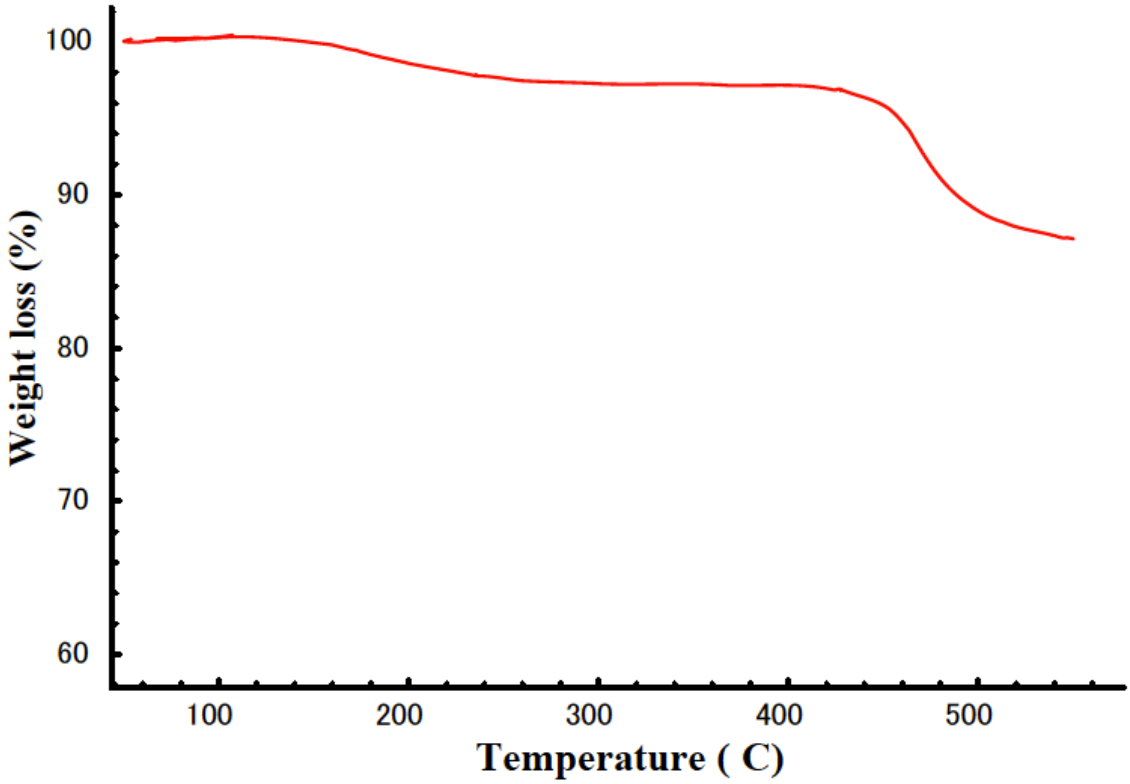

Figure S26. TGA profile of **P2a**; heating rate: 10 ºC/min; N_2 atmosphere

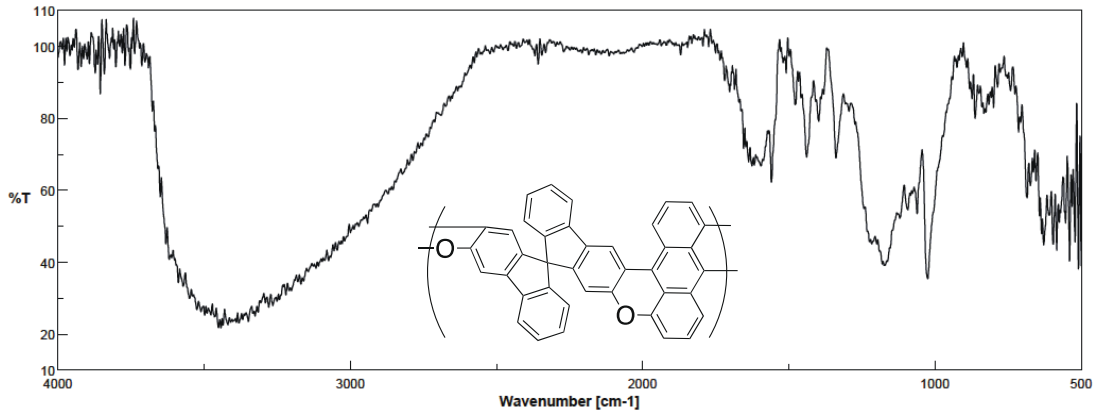

Figure S27. IR spectrum of **P1b** (KBr)

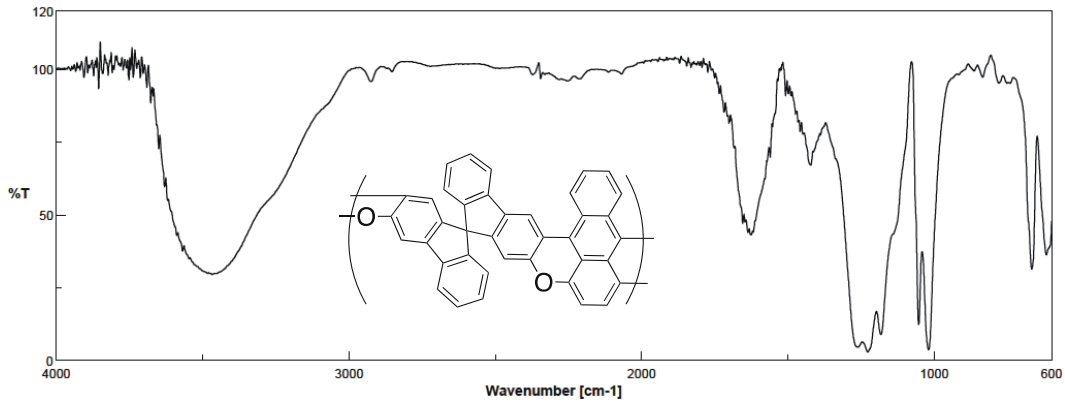

Figure S28. IR spectrum of **P2b** (KBr)

4. UV-vis and CD spectra before and after exposure of P1b and P2b to air

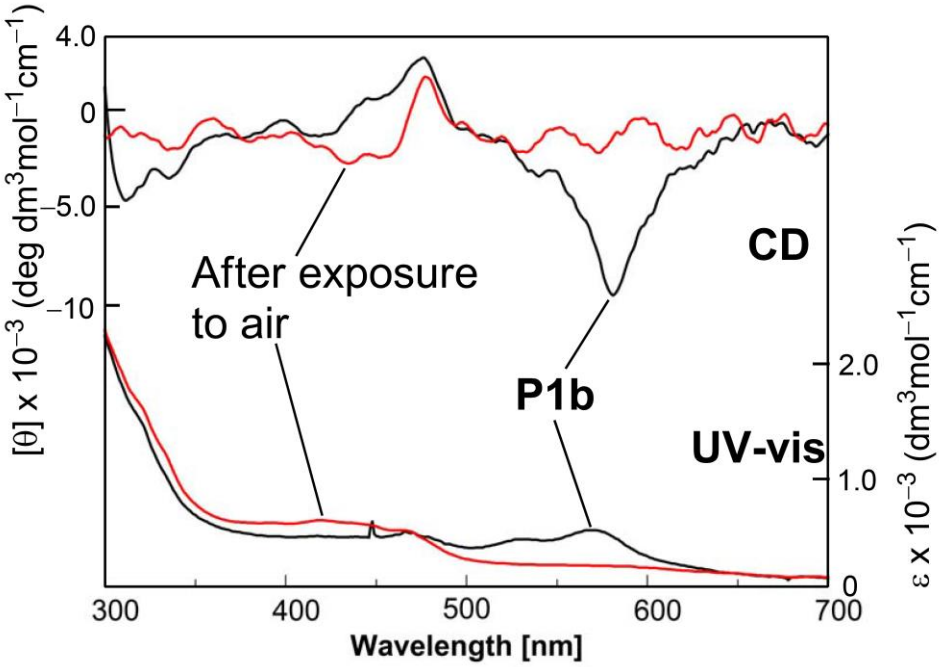

Figure S29. UV-vis and CD spectral change of **P1b** after exposing to air for 1 week. The g_{CD} value of the oxidized polymer was estimated to be 1.6×10^{-4} at 477 nm.

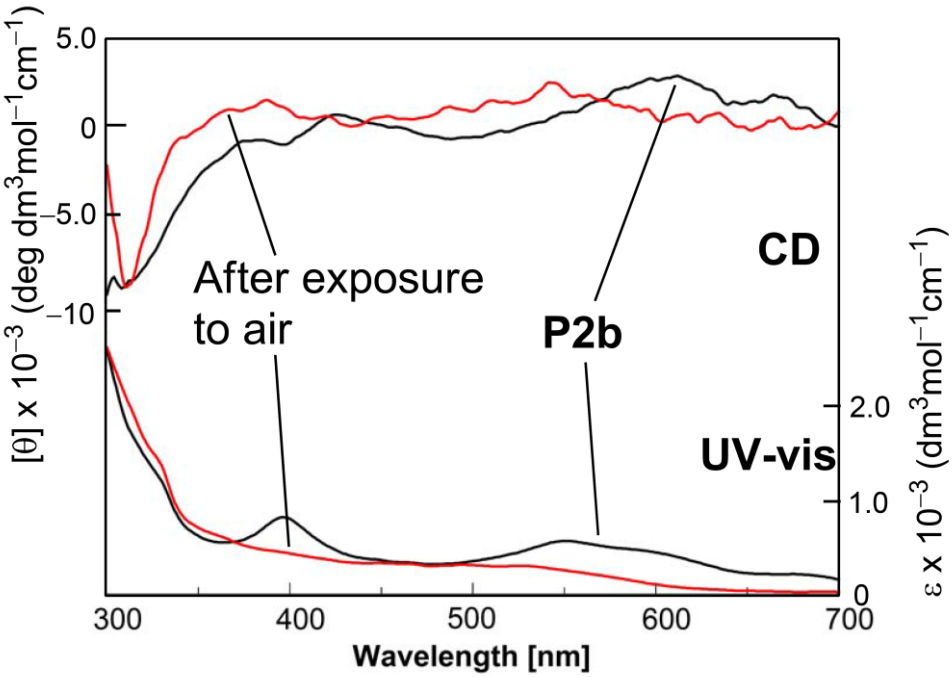

Figure S30. UV-vis and CD spectral change of **P2b** after exposing to air for 1 week. The g_{CD} value of the oxidized polymer was estimated to be 2.5×10^{-4} at 542 nm.

5. Simulated UV-vis and CD spectra of sulfonate-free P1b and P2b in the presence of DMSO using molecular orbital (MO) calculations with a Zerner's intermediate neglect of differential overlap (ZINDO) method in Gaussian 09.[3]

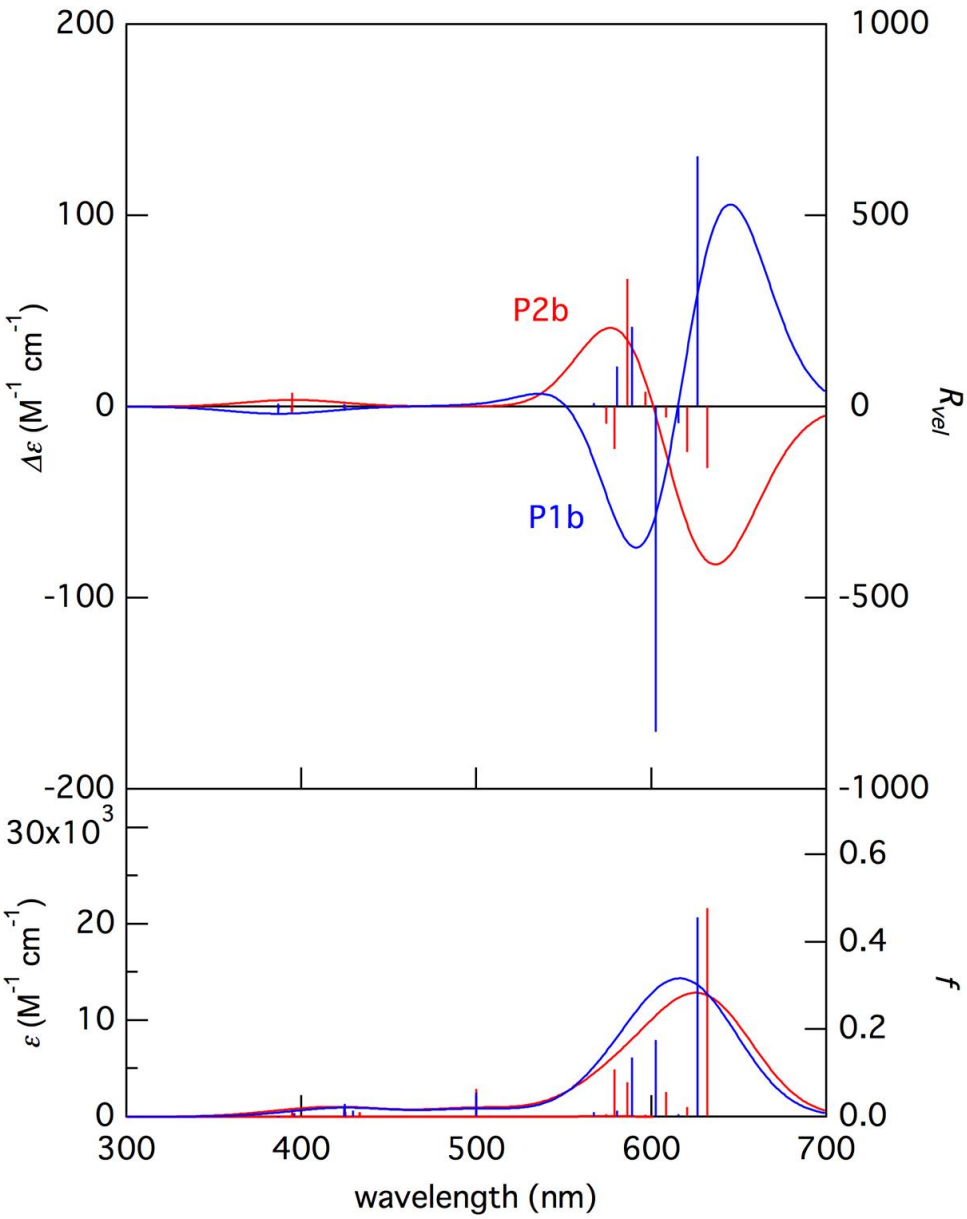

Figure S31. UV-vis and CD spectra of **P1b** and **P2b** simulated by the ZINDO/S (nstates = 20) method using the geometries optimized by OPLS2005.

6. Energy minimized structures of P1a, P2a, P1b, and P2b calculated by OPLS2005

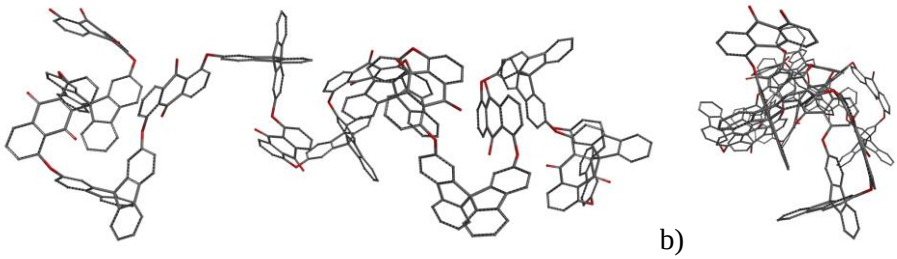

a) b)

Figure S32. Energy-minimized structure of **P1a** calculated by OPLS2005: a) side view and b) front view. Hydrogen atoms are omitted for clarity.

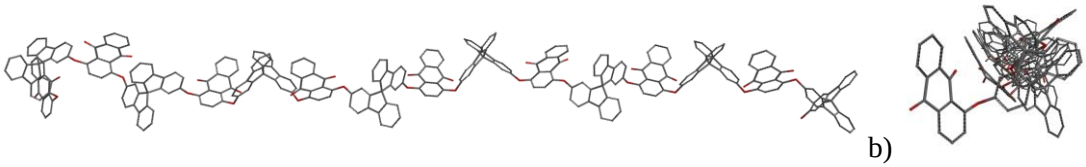

a) b)

Figure S33. Energy-minimized structure of **P2a** calculated by OPLS2005: a) side view and b) front view. Hydrogen atoms are omitted for clarity.

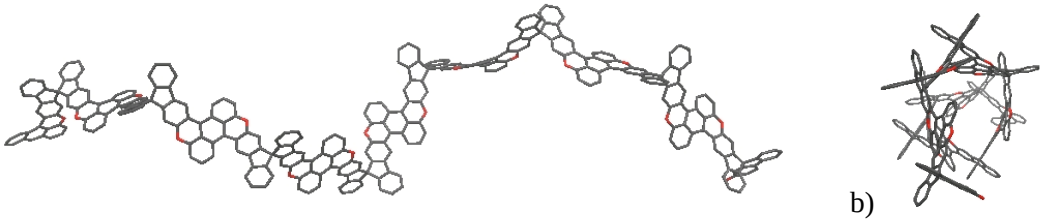

a) b)

Figure S34. Energy-minimized structure of **P1b** calculated by OPLS2005: a) side view and b) front view. Hydrogen atoms are omitted for clarity.

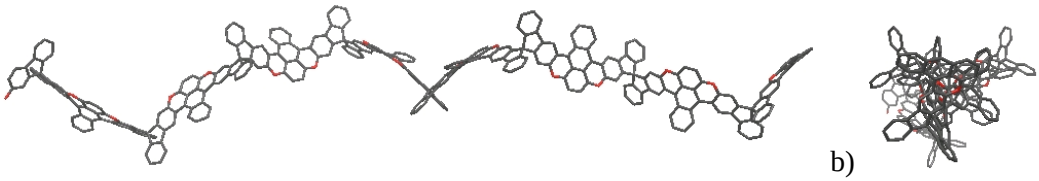

a) b)

Figure S35. Energy-minimized structure of **P2b** calculated by OPLS2005: a) side view and b) front view. Hydrogen atoms are omitted for clarity.

7. References

1) (a) G. Hass, V. Prelog, *Helv. Chim. Acta*., 1969, **52**, 1202. (b) V. Prelog, D. Bedekovic, *Helv. Chim. Acta*., 1979, **62**, 2285. (c) F. Toda, K. Tanaka, *J. Org. Chem*., 1988, **53**, 3607. (d) F. Thiemann, T. Piehler, D. Haase, W. Saak, A. Lützen, *Eur. J. Org. Chem*., 2005, **2005**, 1991.

2) S. Tokita, T. Arai, M. Toya, H. Nishi, *Nippon Kagaku Kaishi*, 1988, 814.

3) (a) M. J. Frisch, G. W. Trucks, H. B. Schlegel, G. E. Scuseria, M. A. Robb, J. R. Cheeseman, G. Scalmani, V. Barone, B. Mennucci, G. A. Petersson, H. Nakatsuji, M. Caricato, X. Li, H. P. Hratchian, A. F. Izmaylov, J. Bloino, G. Zheng, J. L. Sonnenberg, M. Hada, M. Ehara, K. Toyota, R. Fukuda, J. Hasegawa, M. Ishida, T. Nakajima, Y. Honda, O. Kitao, H. Nakai, T. Vreven, J. A. Montgomery, J. E. Peralta, Jr., F. Ogliaro, M. Bearpark, J. J. Heyd, E. Brothers, K. N. Kudin, V. N. Staroverov, T. Keith, R. Kobayashi, J. Normand, K. Raghavachari, A. Rendell, J. C. Burant, S. S. Iyengar, J. Tomasi, M. Cossi, N. Rega, J. M. Millam, M. Klene, J. E. Knox, J. B. Cross, V. Bakken, C. Adamo, J. Jaramillo, R. Gomperts, R. E. Stratmann, O. Yazyev, A. J. Austin, R. Cammi, C. Pomelli, J. W. Ochterski, R. L. Martin, K. Morokuma, V. G. Zakrzewski, G. A. Voth, P. Salvador, J. J. Dannenberg, S. Dapprich, A. D. Daniels, O. Farkas, J. B. Foresman, J. V. Ortiz, J. Cioslowski, D. J. Fox, Gaussian 09, Revision C.01, Gaussian, Inc.: Wallingford CT, 2010. (b) J. E. Ridley, M. C. Zerner, *Theor. Chem. Acc.*, 1973, **32**, 111. (c) J. E. Ridley, M. C. Zerner, *Theor. Chem. Acc.*, 1976, **42**, 223. (d) A. D. Bacon, M. C. Zerner, *Theor. Chem. Acc.*, 1979, **53**, 21. (e) M. C. Zerner, G. H. Loew, R. F. Kirchner, U. T. Mueller-Westerhoff, *J. Am. Chem. Soc.*, 1980, **102**, 589. (f) M. A. Thompson, M. C. Zerner, *J. Am. Chem. Soc.*, 1991, **113**, 8210.